

1 Sulfur-containing particles emitted by concealed sulfide ore deposits: An
2 unknown source of sulfur-containing particles in the atmosphere

3

4 Jianjin Cao^{a,b,*}, Yingkui Li^a, Tao Jiang^a, Guai Hu^a

5 a School of Earth Science and Geological Engineering, Sun Yat-sen University,
6 Guangzhou, People's Republic of China 510275

7 b Guangdong Key Laboratory of Geological Process and Mineral Resources
8 Exploration, Guangzhou, Guangdong 510275, P.R. China

9

10 Abstract

11 Sources of sulfur dioxide, sulfates, and organic sulfur compounds, such as fossil fuels,
12 volcanic eruptions, and animal feeding operations, have attracted considerable
13 attention. In this study, we collected particles carried by geogas flows ascending
14 through soil, geogas flows above the soil that had passed through the soil, and geogas
15 flows ascending through deep faults of concealed sulfide ore deposits and analyzed
16 them using transmission electron microscopy. Numerous crystalline and amorphous
17 sulfur-containing particles or particle aggregations were found in the ascending
18 geogas flows. In addition to S, the particles contained O, Ca, K, Mg, Fe, Na, Pb, Hg,
19 Cu, Zn, As, Ti, Sr, Ba, Si, etc. Such particles are usually a few to several hundred
20 nanometers in diameter with either regular or irregular morphology. The
21 sulfur-containing particles originated from deep-seated weathering or faulting
22 products of concealed sulfide ore deposits. The particles suspended in the ascending

23 geogas flow migrated through faults from deep-seated sources to the atmosphere. This
24 is a previously unknown source of the atmospheric particles. This paper reports, for
25 the first time, the emission of sulfur-containing particles into the atmosphere from
26 concealed sulfide ore deposits. The climatic and ecological influences of these
27 sulfur-containing particles and particle aggregations should be assessed.

28 Keywords: sulfur-containing particles, ascending gas flow, unknown source, sulfide
29 ore deposits.

30 *Corresponding author. Tel.: 862084035033; Fax: 862084035033

31 E-mail address: eescjj@mail.sysu.edu.cn

32

33 1. Introduction

34 Sources of sulfur oxides, sulfates, and organic sulfur compounds are diverse and
35 associated with natural and anthropogenic activities. Known sources of sulfur are
36 volatile sulfur compounds derived from animal feeding operations (Trabue et al.,
37 2008), and aerobic decomposition of food waste (Wu et al., 2010), biogenic sulfur
38 from rice paddies (Yang et al., 1996; Yang et al., 1998) and the Subantarctic and
39 Antarctic Oceans (Berresheim, 1987), sulfur gas (H₂S and SO₂) from geothermal
40 fields (Kristmannsdottir et al., 2000), organic sulfur compounds from sediments and
41 immature crude oil (Sinninghe Damsté et al., 1988), sulfur oxides from the oxidation
42 of fossil fuels (Soleimani et al., 2007), and sulfur dioxide from acid factories and
43 volcanic eruptions (Wong 1978; Sweeney et al., 2008). Sulfate particles, which are
44 important anthropogenic aerosols and influencing climate (Pósfai et al., 1997;
45 Williams et al., 2001). Furthermore, volcanic activity is a major contributor of sulfur
46 to the atmosphere (Zreda-Gostynska et al., 1993; Graf et al., 1998; Streets et al., 2000;
47 Seino et al., 2004; Bhugwant et al., 2009; Bao et al., 2010; Gieré and Querol, 2010),
48 particularly in countries such as Japan, Indonesia, Réunion Island, the Philippines,
49 Iceland, Guatemala, and New Zealand (Rose et al., 1986; Andres et al., 1993; Streets
50 et al., 2000; Seino et al., 2004; Chenet et al., 2005; Bhugwant et al., 2009).

51 Stratospheric sulfur adds very little to the environmental consequences of the
52 anthropogenic sulfur that is released in the troposphere and deposits within days to
53 weeks (Wong, 1978; Chenet et al., 2005). Existing research shows that SO₂ is
54 oxidized to SO₄²⁻ in both the gas and liquid phases. Moreover, sulfate aerosols can

删除的内容: , occur in mineral dust (Kiehl, 1999).

57 directly affect the climate (Graf et al., 1998). In our previous work, particles carried
58 by an ascending geogas flow in the soil (Holub et al., 1999, ~~2001~~; Cao et al., 2009,
59 2010b; Cao et al., 2011; Liu et al., 2011; Wei et al., 2013) were studied and found to
60 contain sulfur. Further research showed that sulfur-containing particles carried by
61 ascending geogas flows can be transported through the soil layers and into the
62 atmosphere. Sulfur-containing particles suspended in the ascending geogas flow
63 migrate through faults from deep-seated concealed sulfide ore deposits to the Earth's
64 surface. These particles are a previously unknown source of sulfur-containing
65 particles in the atmosphere. This paper reports, for the first time, the emission of
66 sulfur-containing particles into the atmosphere from concealed sulfide ore deposits.
67 Because concealed sulfide ore deposits are widely distributed, the influence of
68 sulfur-containing particles derived from them is important. The climatic and
69 ecological effects of these particles should be studied.

70 2. Methods

71 Particles carried by an ascending geogas flow above the soil (that had flown through
72 the soil), in the soil, and in deep-seated faults were collected at the Dongshengmiao
73 polymetallic sulfide deposit in the Inner Mongolia Autonomous Region, China.
74 Particles carried by the ascending gas flow in the soil were also collected at other
75 concealed ore deposits containing sulfide minerals, such as the Kafang copper deposit
76 of the southern Yunnan Province, the Yongshengde copper deposit in northeastern
77 Yunnan, and the Qingmingshan copper–nickel sulfide deposit in Guangxi Province,
78 China.

删除的内容：

80 Particles transported by the ascending geogas flow above the soil (that had flown
81 through the soil) were sampled using stainless steel tubes and carbon-coated nickel
82 transmission electron microscopy (TEM) grids. The length of the stainless steel tubes
83 was 40 cm and their diameter was 2.8 cm. These tubes were inserted vertically into
84 the soil to a depth of about 30 cm. A carbon-coated nickel TEM grid was fixed at the
85 end of the stainless steel tubes. The ascending geogas flow in the soil moved into the
86 stainless steel tubes and naturally passed through the 30 cm soil layer. Then, the gas
87 flow passed through the 10 cm of the empty stainless steel tubes above the soil.
88 Finally, the geogas flow arrived at the top of the tubes. Particles carried by the geogas
89 flow were adsorbed onto the carbon-coated nickel TEM grid. A protective device was
90 installed on the outside of the steel tubes to ensure that particles sampled were those
91 carried by the ascending geogas flow. The protective device is a cylindrical
92 polyethyleneterephthalate bottle. A small hole at the side of the bottle allowed the
93 outflow of ascending geogas flow; however, adsorption material placed in the hole did
94 not allow the external particles to enter. Sampling devices were installed between July
95 25, and August 23, 2013, and the carbon-coated nickel TEM grids were retrieved on
96 September 8, 2013. Sampling sites were distributed across a fault above the concealed
97 sulfide ore bodies of the Dongshengmiao polymetallic sulfide deposit.

98 Particles transported by the ascending geogas flow in the soil were collected using
99 ordinary plastic funnels. An inverted funnel was inserted in a hole that was 60–80 cm
100 deep and backfilled with soil, and a TEM grid was fixed at the end of the funnel spout
101 with nylon net. The setup was protected from contamination using plastic pipes and

102 cups. The TEM grids were retrieved after 60 days.

103 Particles carried by ascending geogas flows in deep-seated faults were sampled using
104 two methods. The first method used an active sampling device with a vacuum pump,
105 polyvinyl chloride (PVC) pipe and carbon-coated nickel TEM grid as the main
106 components. One end of the PVC pipe was connected with a tubing to the pump. A
107 drilling steel was inserted slantwise into the fault. The inserted depth was 30–50 cm.
108 As the drilling steel was pulled out, the PVC pipe was inserted into the hole. The PVC
109 pipe was compacted using fault gouge. The impurity gases in the PVC pipe were
110 pumped out using the vacuum pump, then, the PVC pipe was quickly sealed. A day
111 later, we connected a tube equipped with a carbon-coated nickel TEM grid to the PVC
112 pipe. The gas was pumped using a vacuum pump and flowed through the TEM grid
113 for 1 to 2 hours. Particles carried by the gas were collected by the TEM grid. Finally,
114 the carbon-coated nickel TEM grid was removed and sealed in a sample cell. The
115 second method did not use a vacuum pump. A carbon-coated nickel TEM grid was
116 fixed to the end of the PVC pipe. The ascending geogas flow in the fault flowed into
117 the PVC pipe and arrived at the top of the PVC pipe naturally. The particles carried by
118 the geogas flows in the faults were adsorbed onto the carbon-coated nickel grid. The
119 sampling devices were installed on August 3–10, 2013, and the TEM grids were
120 retrieved on September 7, 2013.

121 High-resolution TEM analyses were performed using a Tecnai G2 F30 S-TWIN
122 instrument at Yangzhou University, China, using an accelerating voltage of 300 kV.
123 The grids were checked using TEM before sampling to ensure they were devoid of

124 particles.

125 3. Results

126 3.1 Sulfur-containing particles carried by an ascending geogas flow above the soil 127 (that had flown through the soil)

128 According to the TEM analysis, particles containing high levels of S, O, Pb, Zn, Fe,
129 Hg, As, etc, were found in the ascending gas flows above the soil above the
130 Dongshengmiao polymetallic sulfide deposit. Table 1 provides the number of
131 sulfur-containing particles or particle aggregations that were found on the 100 μm \times
132 100 μm TEM grid. In general, one aggregation included more than five particles.
133 Figure 1 shows an elliptical particle (ID: 1) having a diameter of 500 nm. The particle
134 contains 78.17% S and 18.47% O (Table 2). Its O to S atomic ratio is 0.47. Figure 2
135 shows a particle aggregation (ID: 2) that consists of several small particles having a
136 diameter of 3–8 nm. It contains 31.23% S and 59.29% Hg. The spacing of the lattice
137 fringes was measured to be 0.333 nm. Figure 3 shows particle aggregations (ID: 3)
138 with sizes of less than 100 nm. Their O to S atomic ratio is 0.51. The particle
139 aggregations contain 14.48% Pb. The particle (ID: 4) illustrated in Figure 4 is
140 elliptical with a diameter of 200 nm and contains 18.55% As, 54.2% Pb, and 8.34%
141 Zn. The particle (ID: 5) shown in Figure 5 contains 2.25% Co. It is amorphous and
142 has an O to S atomic ratio of 2.91. The particle aggregation (ID: 6) illustrated in
143 Figure 6 contains 62.39% Cu and consists of small particles each having a diameter of
144 5–10 nm. Figure 7 presents a particle aggregation (ID: 7) that consists of many small
145 particles with diameters of about 5 nm, and contains 69.28% Pb.

146 3.2 Sulfur-containing particles carried by an ascending gas flow in the soil

147 Numerous sulfur-containing particles transported by an ascending gas flow were
148 found in the soil over sulfide ore deposits. Figure 8 shows an aggregation of such
149 particles from the Dongshengmiao polymetallic sulfide deposit. The aggregation (ID:
150 8) may be composed of CaSO_4 with trace amounts of K, Mg, Fe, and Si. It is regularly
151 shaped and 300 nm in size. The selected area electron diffraction pattern shows that
152 the aggregation is polycrystalline, possibly gypsum. Figure 9 shows a TEM image of
153 a sulfur-containing particle (ID: 9) from the Kafang copper deposit, South China.
154 Sulfur accounts for 63.99% of the particle (Table 3), and its O to S atomic ratio is 0.83.
155 Its K content is 8.93%, and its size is 330 nm. Figure 10 shows a regularly polygonal
156 particle (ID: 10) from the Yongshengde copper deposit, China. Its O to S atomic ratio
157 is 3.60, and its Fe and F contents are 9.94% and 1.71%, respectively. Figure 11 shows
158 a sulfur-containing particle (ID: 11) from the Qingmingshan Cu–Ni sulfide deposit,
159 Guangxi Province, China. Its O to S atomic ratio is 2.51. The particle contains 2.03%
160 Co and is 300 nm \times 400 nm in size. The selected area electron diffraction pattern
161 shows that the particle is amorphous.

162 3.3 Sulfur-containing particles carried by ascending geogas flows in deep-seated 163 faults

164 Sulfur-containing particles were found in samples obtained using two methods from
165 the deep fault gas of the Dongshengmiao polymetallic sulfide deposit. Figure 12
166 shows a sulfur-containing particle aggregation (ID: 12) that was obtained using the
167 vacuum pump from the deep-seated fault gas near a concealed ore body. The

168 aggregation contains O, Na, Si, S, K, Fe, Zn, and Pb. The S content is 23.8%. Figure
169 13 shows a particle aggregation (ID: 13) that was obtained using a PVC pipe from a
170 fault near a concealed ore body. The ascending gas flow arrived at the top of the PVC
171 pipe naturally, and the particles were adsorbed by a TEM nickel grid. The particle
172 aggregation consists of many small particles that are 4–15 nm in diameter. The small
173 particles are elliptical and crystalline, with 0.302 nm spacing of the lattice fringes, and
174 and their main components are O and S. Figure 14 shows a sulfur-containing particle
175 (ID: 14) that was sampled using a PVC pipe in a fault above a concealed ore body.
176 The vertical distance from the sample to the concealed ore body was 85 m. The
177 vertical distance from the sample to the Earth's surface was 230 m.

178 3.4 Sulfur-containing particles in deep-seated fault gouges and oxidized ores

179 Sulfur-containing particles were also found in deep-seated fault gouges and oxidized
180 zones of the Dongshengmiao polymetallic sulfide deposit. For example, Figure 15
181 shows a sulfur-containing particle (ID: 15) from the oxidized zone. According to its
182 atomic percentage, it contains SO_4^{2-} and may be Sr, Ba sulfate, and Ti oxide. Its size
183 is 200 nm \times 400 nm. Figure 16 shows a rhombus-shaped particle (ID: 16) from a
184 deep-seated fault gouge. Its main components are O, S, and Ca, with minor amounts
185 of Fe, Co, and Si.

186 Overall, the sulfur-containing particles or particle aggregations transported by
187 ascending geogas flows can be both regular and irregular in shape and either
188 crystalline or amorphous. The particles or particle aggregations contain Ca, K, Mg, Fe,
189 Na, Pb, Hg, Cu, Zn, As, Ti, Sr, Ba, and Si, as well as O and S.

190 The number of sulfur-containing particles in the ascending geogas flows in
191 non-sulfur-rich areas is much lower than that from the sulfide ore deposits.
192 Furthermore, the overwhelming majority of particles in non-sulfur-rich areas have a
193 low sulphur content. These areas are different from those with the sulfide ore deposits,
194 in which sulfur-containing particles are densely distributed and are present at high
195 levels in the ascending geogas flows.

196 4. Discussion and conclusions

197 Gold particles are formed by post-mineralization fault activity, oxidation, and
198 bacterial weathering of primary minerals (Cao et al., 2010a). Deep-seated gold
199 particles can be transported to the surface by an ascending gas flow, as Brownian
200 motion enables the gold particles in the ascending gas flow to overcome the effect of
201 gravity (Cao et al., 2010a; Cao, 2011). We assume that the same mechanism applies to
202 sulfur-containing particles or particle aggregations. Primary sulfur-containing
203 minerals are transformed into particles by epigenetic reworking, such as
204 post-mineralization fault activity, in which S^{2-} in the sulfide minerals is oxidized to
205 S^{6+} . In this study, the sulfur-containing particles from fault gouges and oxidized ores
206 were found, indicating that these particles were formed by the faulting and oxidation
207 of ores. Faulting and oxidation are well-developed in the Dongshengmiao
208 polymetallic sulfide deposit and other sulfide deposits. This finding indicates that
209 faulting and oxidation play an important role in particle formation.

210 Sulfur-containing particles may be transported to the surface by an ascending geogas
211 flow through faults (Etiope and Martinelli, 2002; Cao et al., 2010a). Material carried

删除的内容: . Because gases and particles
move along faults, they can migrate over
long distances

215 by an ascending geogas flow in the soil in the Xuanhan gas field, Sichuan Province,
216 China was sampled and measured using an instrumental neutron activation analysis.
217 Analysis of trace element anomalies has shown the gas-bearing ring fracture structure
218 to be 4000 m deep, suggesting that particles carried by an ascending geogas flow can
219 be transported over long distances (Yang et al., 2000). The gas flow migrates upward
220 because of the temperature difference and the pressure differences between the Earth's
221 interior and its surface is the reason that the gas flow migrate upward (Tong and Li,
222 1999; Etiope and Martinelli, 2002; Cao et al., 2010a). In this study, Sulfide-containing
223 particles suspended in gas above the soil were found, showing that these particles can
224 move through the soil and get into the atmosphere.

225 The probability that these particles are transported by an ascending geogas flow
226 originating in the soil is low. In the study area, the soil consists of kaolinite, halloysite,
227 montmorillonite, illite, chlorite, hematite, quartz, goethite, and similar minerals.
228 Kaolinite is the main mineral, and the sulfur content in the soil is low. Therefore, this
229 soil is clearly not a probable source of sulfur-containing particles transported by an
230 ascending geogas flow. Furthermore, there is no correlation between the numbers of
231 these particles and those of sulfur-containing particles in the soil solid phase.
232 Sulfur-containing particles are clearly enriched in soils above deep sulfur-rich sources
233 because sulfur-containing particles transported by an ascending geogas flow were
234 found in 16 deep sulfide ore bodies that were studied. This result indicates a close
235 relationship between sulfur-containing particles in the gas flow and deep-seated
236 sulfide ore bodies. Other rock types, such as limestone, siltstone, sandstone, and

删除的内容: the particles or particle aggregations were found in ascending geogas flows in faults at different depths near or above the concealed ore bodies of the Dongshengmiao polymetallic sulfide deposit. This observation demonstrates that the faults are channels for particles carried by the ascending geogas flow.

245 mudstone, do not contain sufficient sulfur to become sources of sulfur-containing
246 particles in an ascending gas flow; for example, the mean sulfur concentrations of the
247 Devonian limestone, mudstone, siltstone, and sandstone in the northern Guangdong
248 Province, China are 610×10^{-6} (68 samples), 80×10^{-6} (25 samples), 160×10^{-6} (33
249 samples), and 110×10^{-6} sulfur (4 samples), respectively.

250 The estimated rate of degassing for the Dongshengmiao deposit calculated to be 2.325
251 $\text{m}^3 \text{s}^{-1}$. The mean sulfur content of the particles carried by the ascending geogas flow
252 for the Dongshengmiao deposit was calculated according to 45 mg/m^3 (Supplement).
253 The estimated annual sulfur emission from particles in the deposit was 3.254 tons. Qi
254 et al. (2007) reported a flue gas amount of $527300 \text{ m}^3 \text{ h}^{-1}$ from the Huhehaote power
255 plant in China and an exit particle concentration of 43.3 mg m^{-3} carried by the flue
256 gas. The SO_3 distribution range in fly ash in 14 power plants (e.g., Tangshan power
257 plant, Gaojing power plant, and Zhengzhou power plant) was reported to range
258 between 0 and 1.05 %. The mean SO_3 and sulfur contents in fly ash were 0.27 % and
259 0.108 %, respectively. On the basis of these mean values, 21.305 tons of annual
260 particulate sulfur emission occurred from the flue gas in the Huhehaote power plant.
261 The annual sulfur emission from the particles carried by ascending geogas flow in the
262 Dongshengmiao deposit was less than carried by the flue gas in the Huhehaote power
263 plant. However, the amount of concealed deposits is much more than that of
264 coal-burning power plants. Moreover, size of the particles carried by the ascending
265 geogas flow from concealed deposits is usually $<500 \text{ nm}$. The mean diameter of the
266 particles carried by the flue gas in 9 samples obtained from four coal-fired power

删除的内容: For 16 ore deposits, in which we have studied particles carried by ascending geogas, a large number of sulfur-containing and Pb- and As-containing particles were found. There are oxidative ore bodies in many concealed sulfide ore deposits. As sulfide minerals change into oxide minerals, sulfide was released from these minerals. There are some sulfide concentration data for ascending geogas. Yuan et al. (China University of Geosciences, Beijing, China, 2014) analyzed sulfide concentrations of ascending geogas in soil at the Sunit deposit (the Inner Mongolia Autonomous Region, China), using plasma mass spectrographic analysis. Their sampling method allowed the flow of geogas in the soil through liquid collector slowly using a pump. The particles carried by the ascending geogas flow were adsorbed in the liquid collector. The volume of the geogas extracted per hole was 5 liters. The geogas extracted from 3 holes (15 liters) was combined to make one sample. The liquid collector was made with high purity nitric acid and Mini-Q ultra pure water. The liquid collector was placed in a 25 ml polyethylene bottle. The analysis results from 1054 samples showed that the average sulfur content of the liquid collector was $26.4571 \mu\text{g ml}^{-1}$. The maximum value was $35.33 \mu\text{g ml}^{-1}$ and the minimum value was $16.89 \mu\text{g ml}^{-1}$. A concentration of $26.4571 \mu\text{g ml}^{-1}$ in the liquid collector may be translated into 44.095 mg per cubic meter of geogas flow. We know that sulfur-containing substances carried by geogas flow may be not completely adsorbed in the liquid collector. Therefore, the average sulfur content of the ascending geogas flow may have been higher than 44.095 mg per cubic meter. We analyzed the sulfide concentration of ascending geogas in the soil at the

365 plants in China were 19.71, 3.18, 5.43, 5.67, 130.94, 77.29, 12.99, 11.59, and 236.63
366 um respectively (Zhang et al. 2007). The sizes of particles carried by the ascending
367 geogas flow from concealed deposits were lesser than those of the particles carried by
368 the flue gas from coal-fired power plants. Within a certain volume, the particles were
369 smaller and the number of particles was more. These small particles are more capable
370 of migration and have a significant health and environmental impact. Therefore,
371 attention must be paid to the particles carried by the ascending geogas flow from
372 concealed deposits.

373 Such sulfur-containing particles enter the atmosphere. Several studies have discussed
374 the direct effects of sulfate particles on the climate (Liu et al., 2009). Some
375 researchers have suggested that sulfur-containing particles can reduce atmospheric
376 temperature or result in climate warming. Streets et al. (2000) suggested that because
377 sulfate aerosols play a vital role in cooling the atmosphere, a reduction in sulfur
378 dioxide emissions in the future would result in increased global warming.
379 Furthermore, aerosol sulfate has been identified as an important contributor to
380 sunlight scattering (Lelieveld and Heintzenberg, 1992; Kim et al., 2001). At the top of
381 the atmosphere above East Asia, SO_4^{2-} radiative forcing is -2 to -10 W m^{-2} over land
382 and -5 to -15 W m^{-2} over ocean (Gao et al., 2014). Niemeier et al. (2011) revealed
383 that an increase in the SO_2 emission rate does not lead to a similar increase in
384 radiative forcing because, as the size of the aerosols increases, their lifetime decreases.
385 It is thus possible that the sulfur-containing particles transported by an ascending
386 geogas flow have an effect on the climate and should, therefore, be evaluated.

删除的内容: The distribution areas of concealed sulfur ore deposits are different. The ore deposits with the distribution areas of 1–12 km² may have more deposits than other areas. Concealed metal deposits containing sulfide minerals can be very extensive, such as the Killik massive sulfide deposit in northeastern Turkey (Çiftçi et al., 2005), the Masa Verde blind massive sulfide deposit in Spain (Ruiz et al., 2002), and the Huize carbonate-hosted Zn–Pb–(Ag) District in South China (Han et al., 2007). Concealed sulfur nonmetallic deposits, such as gypsum and barite, are also widely distributed. The number of concealed sulfide deposits is far greater than those of active volcanoes. Under the climate-warming conditions, oxidation of sulfur-containing minerals is particularly accelerated. .

407 Sulfate particles can be transported into the lungs leading to respiratory illnesses
408 (World Bank Group, 1999; Soleimani et al., 2007). In particular, the sulfur-containing
409 particles contain high levels of toxic Pb, Hg, Cu, and As. In nature, sulfur usually
410 combines with Pb, Hg, Cu, As, Ni, Cd, and Sb, which are toxic to organisms, to form
411 sulfide deposits. The sulfur-containing particles originating from sulfide deposits
412 commonly contain toxic elements. This phenomenon has been confirmed by EDX
413 analysis of particles. The particle sizes carried by the ascending gas flow are usually
414 less than 500 nm. The size is only one-fifth of the upper size limit of PM2.5. Geogas
415 particles undergo long-distance migration. They can remain in the atmosphere for
416 long periods and in can get into bronchioles and alveoli, affecting the ventilative
417 function of lung. They can also enter the blood. The possible relationship between the
418 occurrence of sulfur-containing particles transported by an ascending geogas flow and
419 endemic diseases in the vicinity of sulfur-containing deposits should be investigated.
420 It is probable that sulfur-containing particles transported by the ascending geogas
421 flows in the soil affect the soil system; for example, sulfur-containing particles can
422 affect both soil biota and enzymatic activities, resulting in changes in the soil structure,
423 nutrient cycling, and organic matter decomposition and retention. Sulfur-containing
424 particles may directly catalyze organic matter decomposition. Furthermore, the
425 potential use of such particles as fertilizers for rice plants needs to be investigated.

426 Acknowledgments

427 Financial support from the National Natural Science Foundation of China (Grant Nos.
428 41030425, 41072263, 40773037, and 40673044) and the National High-Tech

删除的内容: have high migration ability
and

431 Research and Development Program of China (863 Program; Grant No.
432 2008AA06Z101) are gratefully acknowledged.

433 References

434 Andres, R. J., Rose, W. I., Stoiber, R. E., Williams, S. N., Mat ías, O., and Morales, R.:

435 A summary of sulfur dioxide emission rate measurements from Guatemalan
436 volcanoes, *B. Volcanol.*, 55, 379–388, 1993.

437 Bao, H. M., Yu, S., and Tong, D. Q.: Massive volcanic SO₂ oxidation and sulphate
438 aerosol deposition in Cenozoic North America, *Nature*, 465, 909–912, 2010.

439 Berresheim H.: Biogenic sulfur emissions from the Subantarctic and Antarctic Oceans,
440 *J. Geophys. Res.*, 92, 13245–13262, 1987.

441 Bhugwant, C., Si ģa, B., Bessafi, M., Staudacher, T., and Eormier, J.: Atmospheric
442 sulfur dioxide measurements during the 2005 and 2007 eruptions of the Piton de
443 La Fournaise volcano: Implications for human health and environmental changes,
444 *J. Volcanol. Geoth. Res.*, 184, 208–224, 2009.

445 Cao, J. J.: Migration mechanisms of gold nanoparticles explored in geogas of the
446 Hetai ore district, southern China, *Geochem. J.*, 45, e9–e13, 2011.

447 Cao, J. J., Hu, R. Z., Liang, Z. R., and Peng, Z. L.: TEM observation of
448 geogas-carried particles from the Changkeng concealed gold deposit, Guangdong
449 Province, South China, *J. Geochem. Explor.* 101, 247–253, 2009.

450 Cao, J. J., Hu, X. Y., Jiang, Z. T., Li, H. W., and Zou, X. Z.: Simulation of adsorption
451 of gold nanoparticles carried by gas ascending from the Earth's interior in
452 alluvial cover of the middle-lower reaches of the Yangtze River, *Geofluids*, 10,

453 438–446, 2010a.

454 Cao, J. J., Liu, C., Xiong, Z. H., and Qin, T. R.: 2010b, Particles carried by ascending
455 gas flow at the Tongchanghe copper mine, Guizhou Province, China, Science
456 China Earth Sciences, 53, 1647–1654, 2010b.

457 Cao, J. J., Liu, C., Zhang, P., Li, Y. P., and Xiong, Z. H.: The characteristic of geogas
458 particles from Daheishan basalt copper deposit in the Huize county of Yunnan,
459 Mital Mine, 113–115, 2011 (in Chinese with English abstract).

460 Chenet, A. L., Fluteau, F., and Courtillot, V.: Modelling massive sulfate aerosol
461 pollution, following the large 1783 Laki basaltic eruption, Earth Planet. Sc. Lett.,
462 236, 721–731, 2005.

463 Etioppe, G., and Martinelli, G., Migration of carrier and trace gases in the geosphere: an
464 overview, Phys. Earth Planet. In., 129, 185–204, 2002.

465 Gao Y., Zhao C., Liu X. H., Zhang, M. G., and Leung, L. R.: WRF-Chem simulations
466 of aerosols and anthropogenic aerosol radiative forcing in East Asia. Atmos.
467 Environ., 92, 250–266, 2014.

468 Gieré R., and Querol, X.: 2010, Atmospheric particles: solid particulate matter in the
469 atmosphere. Elements, 6, 215–222, 2010.

470 Graf, H.-F., Langmann, B., and Feichter, J.: The contribution of Earth degassing to the
471 atmospheric sulfur budget, Chem. Geol., 147, 131–145, 1998.

472 Holub, R. F., Hovorka, J., Reimer, G. M., Honeyman, B. D., Hopke, P. K., and Smrz P.
473 K.: Further investigations of the "geoaerosol" phenomenon, J. Aerosol Sci., 32,
474 61–70, 2001.

删除的内容: Çiftçi, E., Kolaylı, H., and Tokel, S.: Lead-arsenic soil geochemical study as an exploration guide over the Killik volcanogenic massive sulfide deposit, Northeastern Turkey, J. Geochem. Explor., 86, 49–59, 2005. .

Du, L. T.: The new implication about oil-gas origin and outgassing of the earth obtained in Russia, Ukraine, Azerbaijan in new century, Lithologic Reservoirs, 21(4), 1–9, 2009 (in Chinese with English abstract). .

Etioppe, G.: Migrazione e comportamento del "Geogas" in bacini argillosi. Ph.D. Thesis, Dept. Earth Sciences, University of Rome "La Sapienza", Extended abstract in Plinius (1996), 15, 90–94, 1995. .
Etioppe, G.: Subsoil CO₂ and CH₄, and their advective transfer from faulted grassland to the atmosphere, J. Geophys. Res., 104 (D14), 16889–16894, 1999. .

删除的内容: Han, R. S., Liu, C. Q., Huang, Z. L., Chen, J., Ma, D. Y., Lei, L., and Ma, G. S.: Geological features and origin of the Huize carbonate-hosted Zn–Pb–(Ag) District, Yunnan, South China, Ore Geol. Rev., 31, 360–383, 2007. .
Hermansson, H.P., Akerblom, G., Chyssler, J., and Linden, A.: Geogas: A Carrier or a Tracer. SKN Report No. 51. National Board for Spent Nuclear Fuel, Stockholm, 1–66, 1991.

507 Holub, R. F., Reimer, G. M., Hopke, P. K., Hovorka, J., Krčmar, B., and Smrz, P. K.:
508 “Geoaerosols”: their origin, transport and paradoxical behavior: a challenge to
509 aerosol science, *J. Aerosol Sci.*, 30, S111–S112, 1999.

510 Kim, B. G., Park, S. U., and Han, J. S.: Transport of SO₂ and aerosol over the Yellow
511 sea, *Atmos. Environ.*, 35, 727–737, 2001.

512 Kristmannsdóttir, H., Sigurgeirsson, M., Armannsson, H., Hjartarson, H., and
513 Ólafsson, M., Sulfur gas emissions from geothermal power plants in Iceland,
514 *Geothermics*, 29, 525–538, 2000.

515 Lelieveld, J., and Heintzenberg, J.: Sulfate cooling effect on climate through in-cloud
516 oxidation of anthropogenic SO₂, *Science*, 258, 117–120, 1992.

517 Liu, C., Cao, J. J., and Ke, H. L.: Geogas characteristic of Yongshengde copper ores in
518 the Northeastern Yunnan, China, *Geology of Chemical Minerals*, 33, 201–207,
519 2011(in Chinese with English abstract).

520 Liu, Y., Sun, J. R., and Yang, B.: The effects of black carbon and sulfate aerosols in
521 China regions on East Asia monsoons, *Tellus B*, 61, 642–656, 2009.

522 Niemeier, U., Schmidt, H., and Timmreck, C.: The dependency of geengineered
523 sulfate aerosol on the emission strategy, *Atmos. Sci. Lett. Special Issue:
524 Geoengineering*, 12, 189–194, 2011.

525 Pósfai, M., Anderson, J. R., and Buseck, P. R.: Soot and sulfate aerosol particles in the
526 remote marine atmosphere, in: Geological Society of America, 1997 annual
527 meeting, Abstracts with Programs - Geological Society of America, 29, 357,
528 1997.

删除的内容: Judd, A. G., Davies, J.,
Wilson, J., Holmes, R., Baron, G., and
Bryden, I.: Contributions to atmospheric
methane by natural seepages on the UK
continental shelf, *Mar. Geol.*, 137, 165–189,
1997. .
Kiehl, J. T.: Solving the aerosol puzzle,
Science, 283, 1273–1275, 1999. .

删除的内容: Malmqvist, L. and
Kristiansson, K.: Experimental evidence for
an ascending micro-flow of geogas in the
ground, *Earth Planet. Sc. Lett.*, 70, 407–423,
1984. .
Märner, N.-A. and Etiope, G.: Carbon
degassing from the lithosphere, *Global
Planet. Change*, 33, 185–203, 2002. .

545 [Qi, L. Q., Yuan, Y.T., and Liu, J.: Current situations of emission and collection on fly](#)
546 [ash of power plants in China: International Conference on Power](#)
547 [Engineering-2007, Hangzhou, China, 23 – 27 October 2007, 766 – 772, 2007.](#)

548 Rose, W. I., Chuan, R. L., Giggenbach, W. F., Kyle, P. R., and Symonds, R. B.: Rates
549 of sulfur dioxide and particle emissions from White Island volcano, New
550 Zealand, and an estimate of the total flux of major gaseous species, *B. Volcanol.*,
551 48, 181–188, 1986.

552 [Seino, N., Sasaki, H., Sato, J., and Chiba, M.: High-resolution simulation of volcanic](#)
553 [sulfur dioxide dispersion over the Miyake Island, *Atmos. Environ.*, 38,](#)
554 [7073–7081, 2004.](#)

删除的内容: Ruiz, C., Arribas, A., and Arribas, Jr., A.: Mineralogy and geochemistry of the Masa Valverde blind massive sulphide deposit, Iberian Pyrite Belt (Spain), *Ore Geol. Rev.*, 19, 1–22, 2002. .

555 Sinninghe Damsté J. S., Irene, W., Rijpstra, C., de Leeuw, J. W., and Schenck, P. A.:
556 1988, Origin of organic sulfur compounds and sulfur-containing high molecular
557 weight substances in sediments and immature crude oils, *Org. Geochem.*, 13,
558 593–606, 1988.

559 Soleimani, M., Bassi, A., and Margaritis A.: Biodesulfurization of refractory organic
560 sulfur compounds in fossil fuels, *Biotechnol. Adv.*, 25, 570–596, 2007.

561 Streets, D. G., Tsai, N. Y., Akimoto, H., and Oka, K.: Sulfur dioxide emissions in Asia
562 in the period 1985–1997, *Atmos. Environ.*, 34, 4413–4424, 2000.

563 Sweeney, D., Kyle, P. R., and Oppenheimer, C.: Sulfur dioxide emissions and
564 degassing behavior of Erebus volcano, Antarctica, *J. Volcanol. Geoth. Res.*, 177,
565 725–733, 2008.

566 Tong, C. H., and Li, J. C.: A new method searching for concealed mineral resources:

573 geogas prospecting based on nuclear analysis and accumulation sampling, J.
574 China Univ. Geosci., 10, 329–332, 1999.

575 Trabue, S., Scoggin, K., Mitloehner, F., Li, H., Burns, R., and Xin, H. W.: Field
576 sampling method for quantifying volatile sulfur compounds from animal feeding
577 operations, Atmos. Environ., 42, 3332–3341, 2008.

578 Wei, X. J., Cao, J. J., Holub, R. F., Hopke, P. K., and Zhao, S. J.: TEM study of
579 geogas-transported nanoparticles from the Fankou Lead-Zinc Deposit,
580 Guangdong Province, South China, J. Geochem. Explor., 128, 124–135, 2013.

581 Williams, K. D., Jones, A., Roberts, D. L., Senior, C. A., and Woodage, M. J.: The
582 response of the climate system to the indirect effects of anthropogenic sulfate
583 aerosol, Clim. Dynam., 17, 845–856, 2001.

584 Wong, M. H.: An ecological survey of the effect of sulfur dioxide emitted from an
585 Acid Work Factory, B. Environ. Contam. Tox., 19, 715–723, 1978.

586 World Bank Group: Pollution prevention and abatement handbook: towards cleaner
587 production, World Bank Group Publishers, Washington DC, 1999, 1998.

588 Wu, T., Wang, X. M., Li, D. J., and Yi, Z. G.: Emission of volatile organic sulfur
589 compounds (VOSCs) during aerobic decomposition of food wastes, Atmos.
590 Environ., 44, 5065–5071, 2010.

591 Yang, F. G., and Tong, C. H.: Geogas anomaly and mechanism in Xuanhan gas field,
592 Earth Science-Journal of China University of Geosciences, 2000, 25, 103–106
593 (in Chinese with English abstract).

594 Yang, Z., Kanda, K., Tsuruta, H., and Minami, K.: Measurement of biogenic sulfur

595 gases emission from some Chinese and Japanese soils, Atmos. Environ., 30,
596 2399–2405, 1996.

597 Yang, Z., Kong, U. L., Zhang, J., Wang, L., and Xia, S.: Emission of biogenic sulfur
598 gases from Chinese rice paddies, Sci. Total Environ., 224, 1–8, 1998.

599 Zhang, C. F, Yao, Q., and Sun, J. M.: Characteristics of particulate matter from
600 emissions of four typical coal-fired power plants in China, Fuel Process Technol.,
601 86, 757– 768, 2005.

602 Zreda-Gostynska, G., Kyle, P., and Finnegan, D.: Chlorine, fluorine, and sulfur
603 emissions from Mount Erebus, Antarctica and estimated contributions to the
604 Antarctic atmosphere, Geophys. Res. Lett., 20, 1959–1962, 1993.

605

606

607

608

609

610

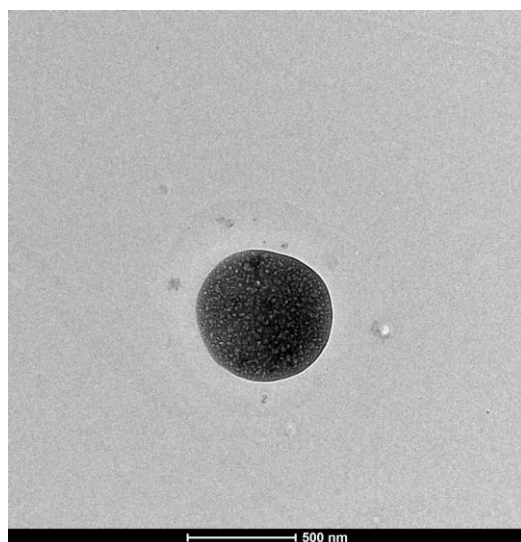
611

删除的内容: Yuan, L. L., Wang, M. Q.,
and Hu, J. L.: Research of geochemical gas
prospecting in sunit, Coal Technology, 33,
85–87, 2014 (in Chinese with English
abstract).

617

618

619



620 Fig. 1 TEM image of an S-, O-, and Si-containing particle obtained from an ascending
621 gas flow above the soil over the Dongshengmiao deposit.

622

623

624

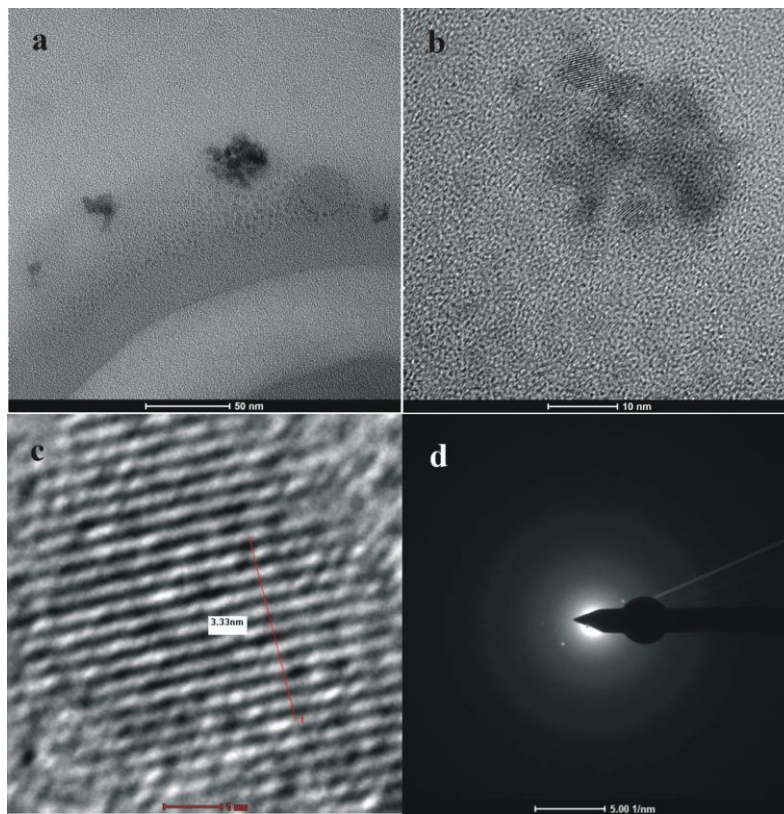
625

626

627

628

629



630 Fig. 2(a) TEM image, (b, c) high-resolution (HRTEM) images, and (d) selected area
631 electron diffraction (SAED) pattern of an S-, O-, Hg-containing particle aggregation
632 obtained from an ascending gas flow above the soil over the Dongshengmiao deposit.

633

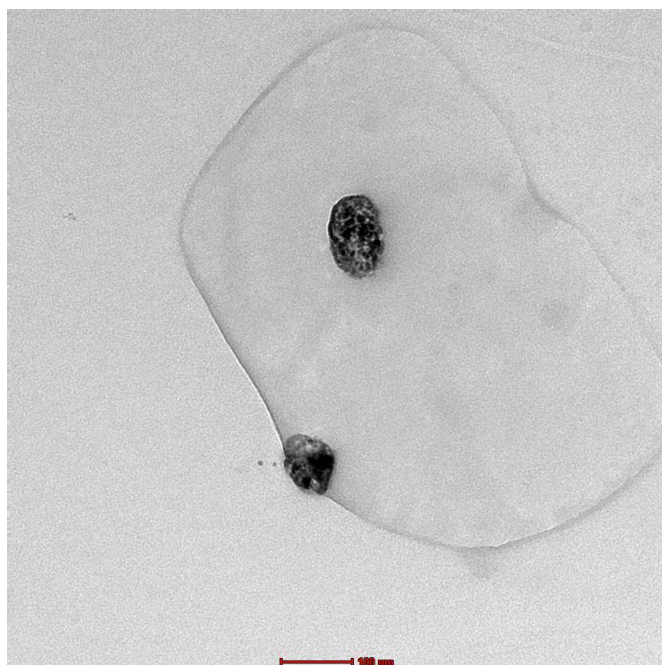
634

635

636

637

638



639

640 Fig. 3 TEM image of S-, O-, K-, and Pb-containing particle aggregations obtained

641 from an ascending gas flow above the soil over the Dongshengmiao deposit.

642

643

644

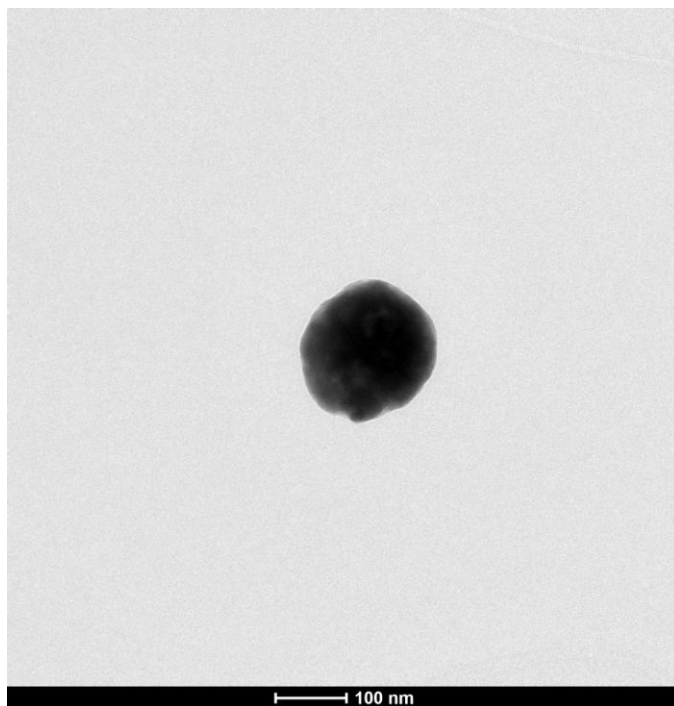
645

646

647

648

649



650

651

652 Fig. 4 TEM image of an S-, O-, Na-, Pb-, Zn-, and As-containing particle obtained
653 from an ascending gas flow above the soil over the Dongshengmiao deposit.

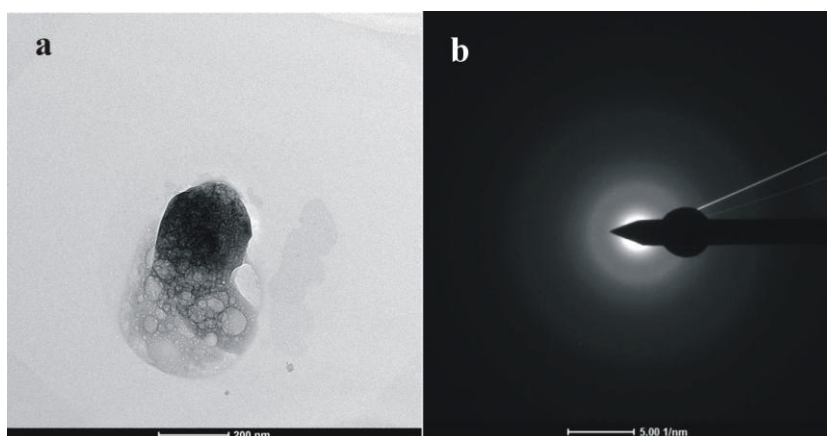
654

655

656

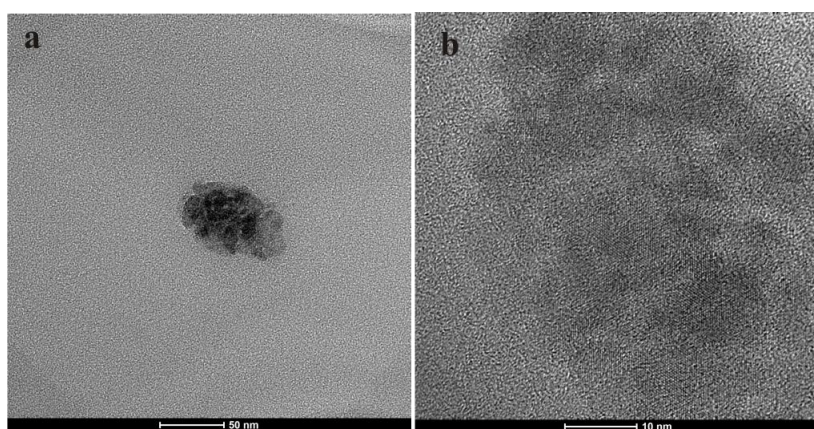
657

658



659 Fig. 5 (a) TEM image and (b) SAED pattern of an S-, O-, K-, Na-, and Pb-containing
 660 particle obtained from an ascending gas flow above the soil over the Dongshengmiao
 661 deposit.

662



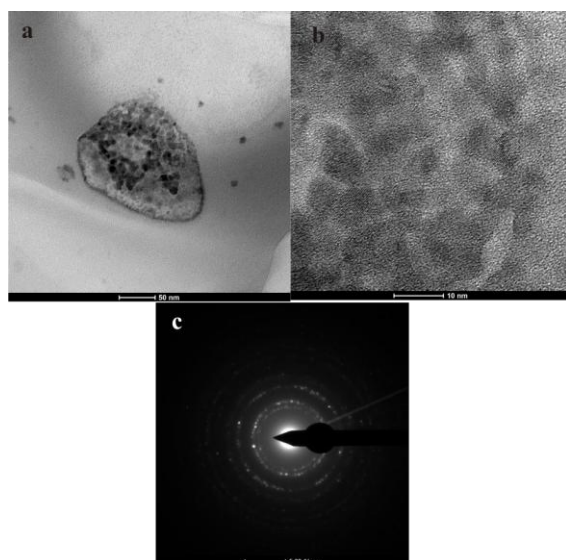
663 Fig. 6 (a) TEM image and (b) HRTEM image of an O-, Si-, S-, and Cu-containing
 664 particle aggregation obtained from an ascending gas flow above the soil over the
 665 Dongshengmiao deposit.

666

667

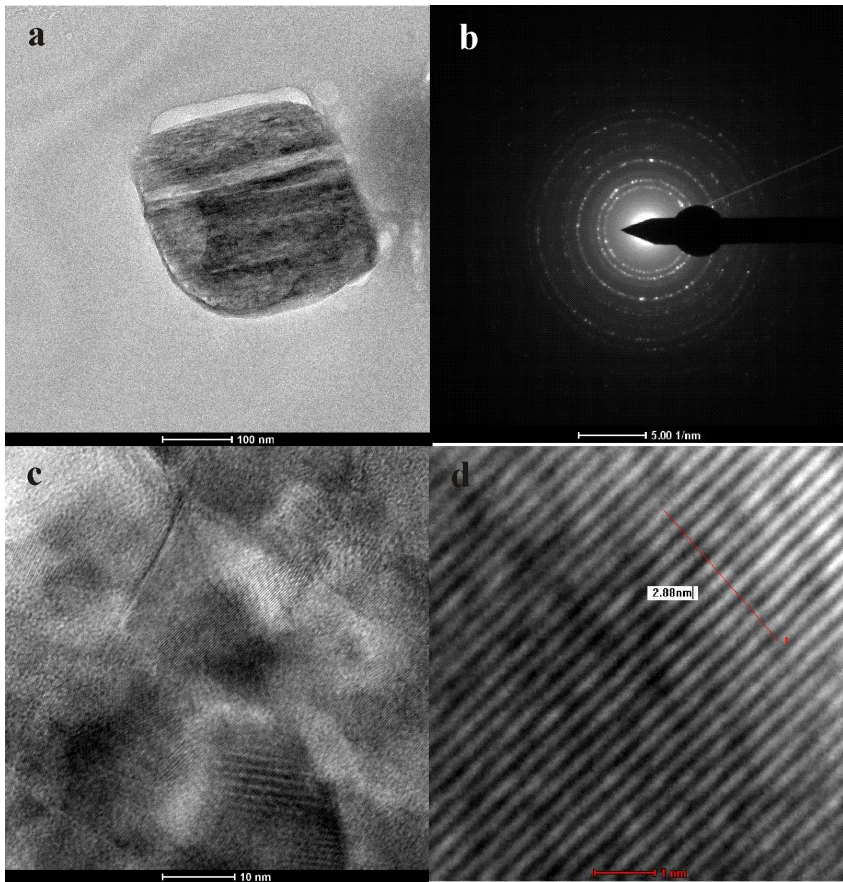
668

669 |
670
671



672 Fig. 7 (a) TEM image, (b)HRTEM image, and (c) SAED pattern of an O-, S-, K-, and
673 Pb-containing particle aggregation obtained from an ascending gas flow above the
674 soil over the Dongshengmiao deposit.

675
676
677
678
679
680
681
682
683
684
685
686
687
688
689
690
691
692



693

694 Fig. 8 (a) TEM image, (b) SAED pattern, and (c, d) HRTEM image of an O-, S-, Ca-,
695 and Mg-containing particle obtained from an ascending gas flow in the soil over
696 Dongshengmiao deposit.

697

698

699

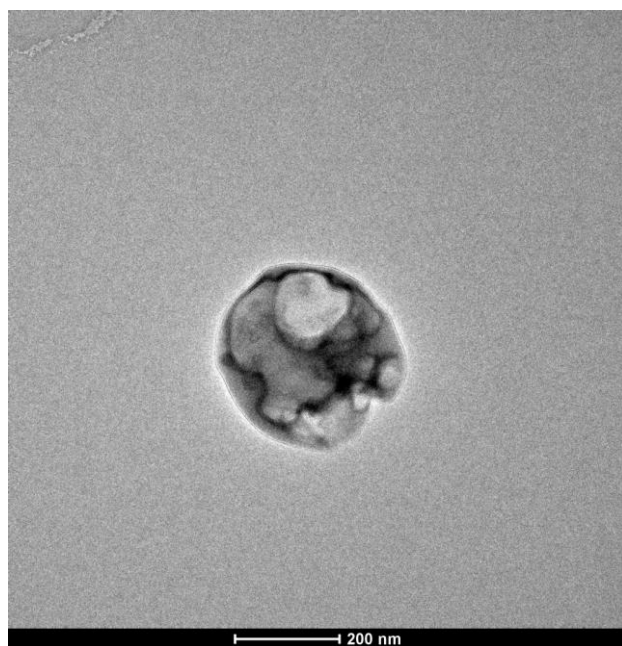
700

701

702

703

704



705

706 Fig. 9 TEM image of an O-, S-, and K-containing particle obtained from an ascending
707 gas flow in the soil from the Kafang copper deposit, Yunnan Province.

708

709

710

711

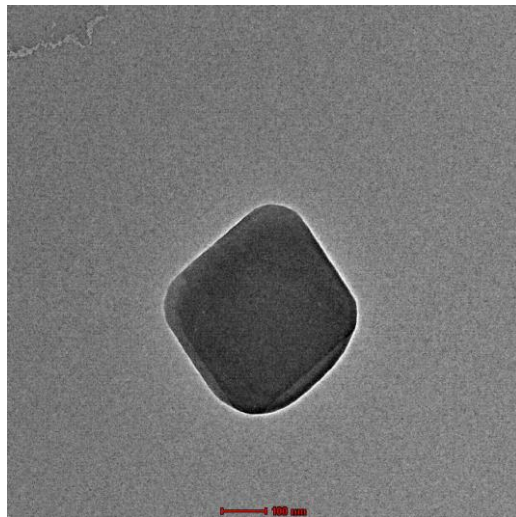
712

713

714

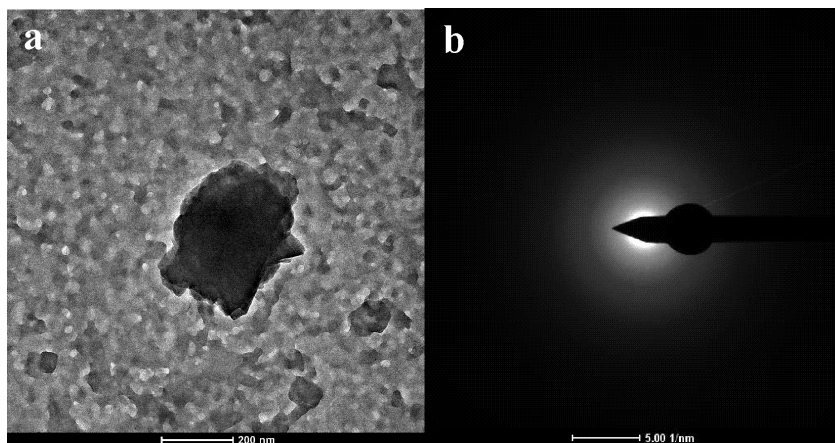
715

716



717 Fig. 10 TEM image of an O-, S-, and Fe-containing particle obtained from an
718 ascending gas flow in the soil from the Yongshengde copper deposit in northeastern
719 Yunnan.

720



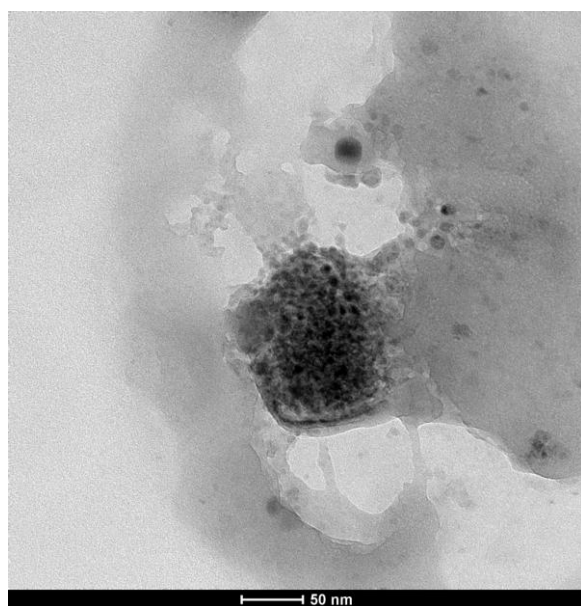
721 Fig. 11 (a) TEM image and (b) SAED pattern of an O-, S-, and Co-containing particle
722 obtained from an ascending gas flow in the soil from the Qingmingshan Cu–Ni
723 sulfide deposit, Guangxi Province.

724

725

726

727



728

729 Fig. 12 TEM image of an O-, S-, K-, Pb-, and Na-containing particle sampled using a
730 vacuum pump from the fault gas near a concealed ore body of the Dongshengmiao
731 deposit.

732

733

734

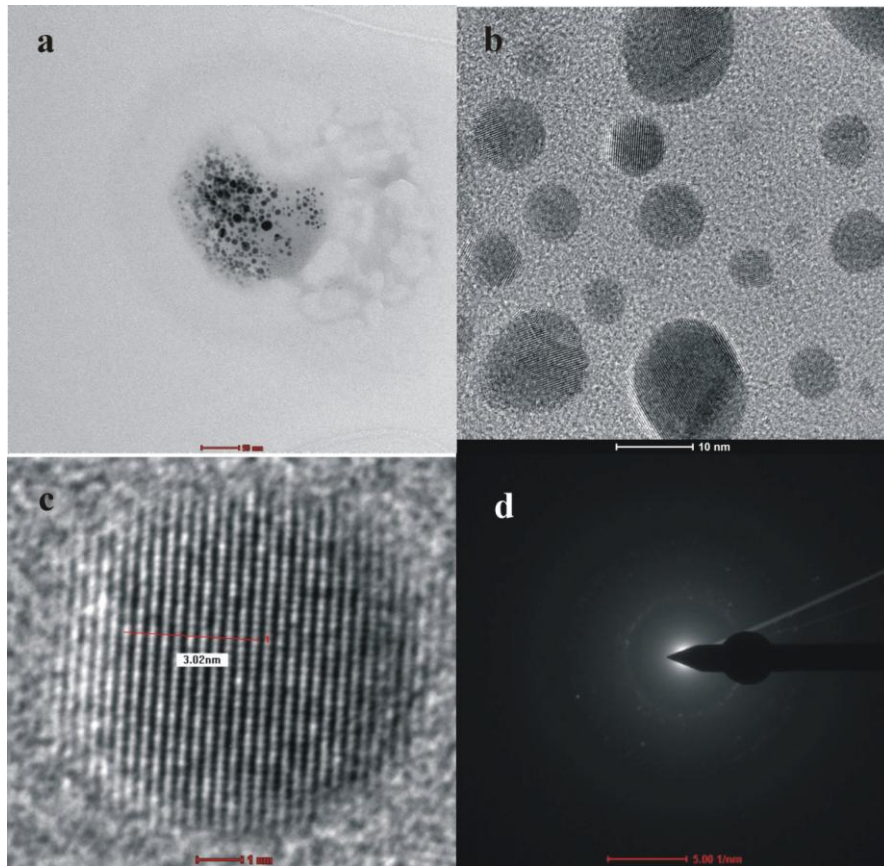
735

736

737

738

739



740

741 Fig. 13 (a) TEM image, (b, c) HRTEM images, and (d) SAED pattern of an O-, S-,
742 and K-containing particle aggregation sampled using a PVC pipe in a fault near a
743 concealed ore body of the Dongshengmiao deposit.

744

745

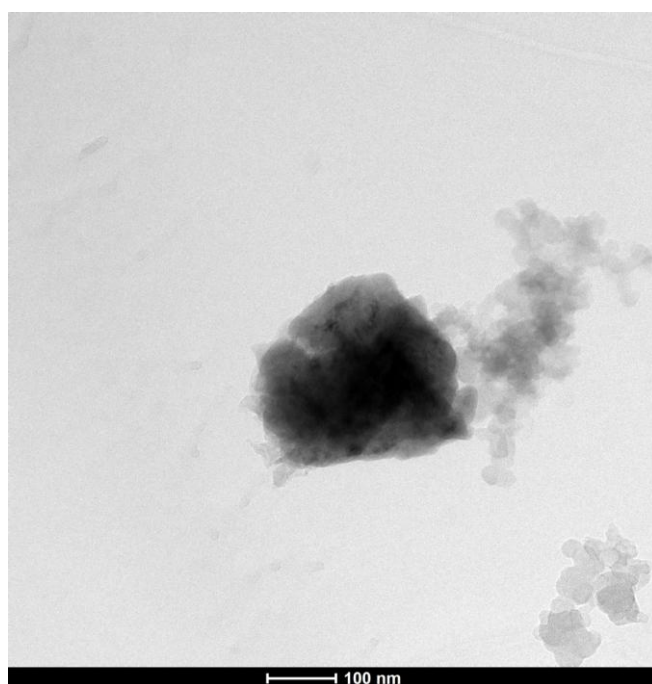
746

747

748

749

750



751

752

753 Fig. 14 TEM image of an O-, S-, Fe-, and Mg-containing particle aggregation
754 sampled using a PVC pipe in a fault above a concealed ore body of the
755 Dongshengmiao deposit.

756

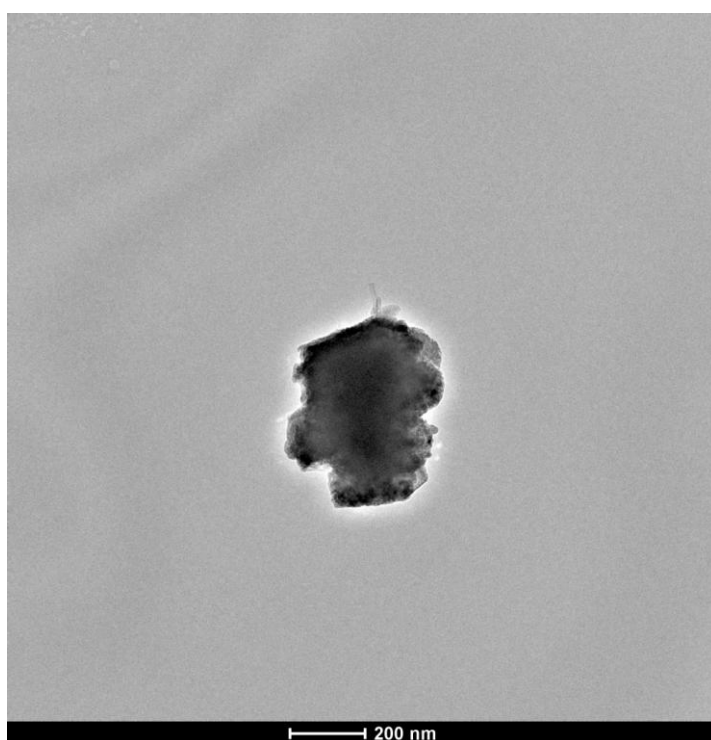
757

758

759

760

761



762

763 Fig. 15 TEM image of an O-, S-, Ti-, Sr-, and Ba-containing particle from a
764 deep-seated oxidized zone in the Dongshengmiao deposit.

765

766

767

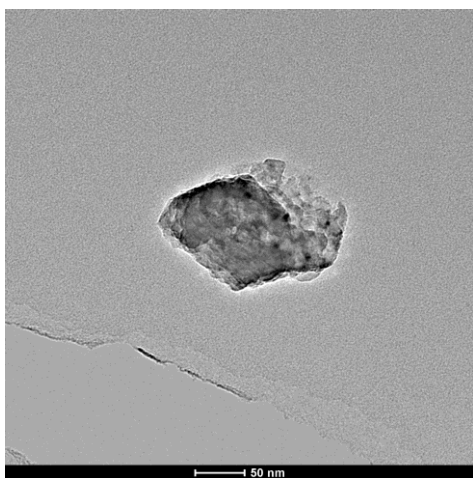
768

769

770

771

772



773

774

775 Fig. 16 TEM image of an O-, S-, Fe-, Co-, and Ca-containing particle from a
776 deep-seated fault gouge in the Dongshengmiao deposit.

777

778

779

780

781

782

783

784

785

786

787

788

789

790
791
792
793
794
795

Table 1 Number of sulfur-containing particles or particle aggregations number from the Dongshengmiao deposit on 100 μm × 100 μm TEM grids

Sulfur-containing particles or particle aggregations carried by ascending gas flow above the soil (that had flown through the soil)				Sulfur-containing particles or particle aggregations carried by ascending gas flow in deep faults			
Sample	Sample box	Grid	Number	Sample	Sample box	Grid	Number
ND13-1	A1	A1-1	3	NDDW03	A2	A2-2	3
ND13-2	A2	A2-1	2	NDDW05	A4	A4-1	1
ND13-3	A3	A3-2	1			A4-2	29
		A3-3	6	NDDW06	A5	A5-2	1
ND13-4	A4	A4-1	1	NDDW07	B1	B1-1	4
		A4-2	2			B1-2	1
ND13-6	A5	A5-1	1	NDDW19	D3	D3-2	1
		A5-2	3			D3-3	2
		A5-3	1	NDDW26	E4	E4-1	1
ND13-8	B2	B2-1	1			E4-3	1
		B2-2	6	NDDW27	E5	E5-1	2
		B2-3	1			E5-3	2
ND13-9	B3	B3-1	1			E5-4	1
		B3-2	1	NDDW36	G4	G4-1	12
		B3-3	1			G4-3	10
ND13-10	B4	B4-1	1			G4-4	1
		B4-3	6	NDDW37	G5	G5-1	1
ND13-11	B5	B5-1	1				

796
797
798
799
800
801
802
803
804
805
806
807
808
809

810
 811
 812
 813
 814
 815

Table 2 EDX results for particles 1–8.

Element	Particle number							
	1	2	3	4	5	6	7	8
Weight O%	18.47	9.46	16.02	9.73	15.75	12.9	5.13	51.88
Atomic O%	31.1	31.78	31.12	39.3	34.16	31.35	22.74	69.78
Weight Si%	3.35		1.49	0.5	1.09	3.08		2.19
Atomic Si%	3.21		1.65	1.15	1.34	4.27		1.67
Weight S%	78.17	31.23	63.1	3.82	10.83	21.61	18.25	19.02
Atomic S%	65.68	52.33	61.16	7.7	11.72	26.2	40.32	12.76
Weight Hg%		59.29						
Atomic Hg%		15.87						
Weight K%			4.88		35.75		7.31	0.99
Atomic K%			3.88		31.73		13.25	0.54
Weight Pb%			14.48	54.2	22.5		69.28	
Atomic Pb%			2.17	16.9	3.76		23.67	
Weight Na%				3.1	9.66			
Atomic Na%				8.73	14.58			
Weight Fe%				0.75	2.14			0.21
Atomic Fe%				0.87	1.33			0.08
Weight Co%				0.98	2.25			
Atomic Co%				1.08	1.32			
Weight Zn%				8.34				
Atomic Zn%				8.24				
Weight As%				18.55				
Atomic As%				16				
Weight Cu%						62.39		
Atomic Cu%						38.16		
Weight Mg%								3.86
AtomicMg%								3.42
Weight Ca%								21.82
Atomic Ca%								11.71

816
 817
 818
 819
 820
 821
 822
 823

824
825
826
827
828

Table 3 EDX results for particles 9–16.

Element	Particle number							
	9	10	11	12	13	14	15	16
Weight O%	26.54	56.25	53.66	25.39	67.03	17.21	29.21	40.8
Atomic O%	42.51	73.54	70.2	37.32	80.72	35.83	64.85	62.97
Weight Si%	0.52			0.66	1	0.7		1.5
Atomic Si%	0.47			0.55	0.68	0.83		1.32
Weight S%	63.99	31.3	42.81	23.8	28.01	24.59	10.88	15.03
Atomic S%	51.15	20.42	27.95	17.45	16.83	25.53	12.05	11.58
Weight K%	8.93	0.78		2.01	2.59			
Atomic K%	5.85	0.42		1.21	1.27			
Weight Pb%				4.25				
Atomic Pb%				0.48				
Weight Na%			1.04	40.92		1.35		
Atomic Na%			0.95	41.84		1.96		
Weight Fe%		9.94	0.44	1.11	1.35	51.16	1.27	5.2
Atomic Fe%		3.72	0.16	0.46	0.46	30.5	0.81	2.3
Weight Co%			2.03					6.36
Atomic Co%			0.72					2.66
Weight Zn%				1.82				
Atomic Zn%				0.65				
Weight Mg%						2.74		
Atomic Mg%						3.75		
Weight Ca%						0.28	0.5	31.08
Atomic Ca%						0.23	0.44	19.15
Weight F%		1.71						
Atomic F%		1.88						
Weight Al%						0.25		
Atomic Al%						0.3		
Weight Mn%						1.68		
Atomic Mn%						1.02		
Weight Ti%							10.94	
Atomic Ti%							8.11	
Weight Sr%							10.32	
Atomic Sr%							4.18	
Weight Ba%							36.86	
Atomic Ba%							9.53	

829
830
831

832
833
834
835
836
840
841
842
843
844
845
846
847
848
849
850
851
852
853
854
855
856
857
858
859
860
861
862
863
864
865
866
867
868
869
870
871
872
873
874
875
876
877
878

删除的内容: Table 4 Plasma spectrum S
results for liquid collectors along the 1st
section (µg/mL) .
Number

883 *Supplement of*

884 **Sulfur-containing particles emitted by concealed sulfide ore deposits:**

885 **An unknown source of sulfur-containing particles in the atmosphere**

886 **Jianjin Cao et al.**

887 *Correspondence to:* Jianjin Cao (eescjj@mail.sysu.edu.cn)

888

889

890

891

892

893

894

895

896

897

898

899

900

901

902

903

904

Supplementary Information

905

906 For 16 ore deposits, in which we have studied particles carried by ascending geogas, a
907 large number of sulfur-containing and Pb- and As-containing particles were found.
908 There are oxidative ore bodies in many concealed sulfide ore deposits. As sulfide
909 minerals change into oxide minerals, sulfide was released from these minerals. There
910 are some sulfide concentration data for ascending geogas. Yuan et al. (China
911 University of Geosciences, Beijing, China, 2014) analyzed sulfide concentrations of
912 ascending geogas in soil at the Sunit deposit (the Inner Mongolia Autonomous Region,
913 China), using plasma mass spectrographic analysis. Their sampling method allowed
914 the flow of geogas in the soil through liquid collector slowly using a pump. The
915 particles carried by the ascending geogas flow were adsorbed in the liquid collector.
916 The volume of the geogas extracted per hole was 5 liters. The geogas extracted from 3
917 holes (15 liters) was combined to make one sample. The liquid collector was made
918 with high purity nitric acid and Mini-Q ultra pure water. The liquid collector was
919 placed in a 25 ml polyethylene bottle. The analysis results from 1054 samples showed
920 that the average sulfur content of the liquid collector was $26.4571 \mu\text{g ml}^{-1}$. The
921 maximum value was $35.33 \mu\text{g ml}^{-1}$ and the minimum value was $16.89 \mu\text{g ml}^{-1}$. A
922 concentration of $26.4571 \mu\text{g ml}^{-1}$ in the liquid collector may be translated into 44.095
923 mg per cubic meter of geogas flow. We know that sulfur-containing substances
924 carried by geogas flow may be not completely adsorbed in the liquid collector.
925 Therefore, the average sulfur content of the ascending geogas flow may have been
926 higher than 44.095 mg per cubic meter. We analyzed the sulfide concentration of

927 ascending geogas in the soil at the Kangjiawan deposit in the Hunan Province, China.
928 Our sampling method is similarly to the method used by Yuan et al. (2014). The main
929 difference is that our liquid collector was made with high purity aqua regia and
930 tri-distilled water. The volume of the liquid collector was 100 ml. The volume of the
931 geogas extracted from a hole was 9 liters. Therefore, the volume of the geogas
932 extracted from 3 holes was 27 liters. The sulfide concentration of the liquid collector
933 was analyzed using the plasma spectrum method. We analyzed the samples along 3
934 sections (sample numbers were 31, 74, and 20). The results showed that the average
935 sulfur contents of the 3 sections were 0.27, 1.40, and 32.81 $\mu\text{g ml}^{-1}$ respectively
936 (Tables S1–3), which may be translated into 1.00, 5.19, and 121.50 mg per cubic
937 meter of geogas flow, respectively. [Wang et al. \(2008\) collected particles carried by](#)
938 [ascending geogas in soil over the Jiaolongzhang Pb-Zn-Cu-Ag deposit, Eastern Gansu,](#)
939 [China using a liquid collector. Analysis results from 14 samples showed that the mean](#)
940 [content of Cu, Pb, and Zn was 844 ng/ml \(gas volume\), 107 ng/ml, and 1751 ng/ml,](#)
941 [respectively.](#)

942 There is earth degassing phenomena in metallic and nonmetallic deposits. The giant
943 gold deposits, such as the Porcupine gold deposit in Canada, the Witwatersrand gold
944 deposit in South Africa, and the Muruntau gold deposit in Uzbekistan, exhibit upward
945 vertical movement of hydrocarbon gas. The Witwatersrand gold deposit has
946 significant upward gas flow. In one day, 36700 m^3 of hydrocarbon gases degas from
947 underground gold mining vents and $5 \times 10^8 \text{ m}^3$ of hydrocarbon gases degas from
948 3000m or deeper mines every year. The Azerbaijan oil and gas region is strongly

949 degassed, with $4 \times 10^8 \text{ m}^3$ of gases degassed every year (Du, 2009). The ascending
950 gas flow rates were measured to be between 60×10^{-4} and $4 \text{ cm}^3 \text{ min}^{-1} \text{ m}^{-2}$
951 horizontally projected borehole area at three different sites by Malmqvist &
952 Kristiansson (1984). Carbon dioxide concentrations above sulfide mineralizations are
953 often enhanced. Hidden sulfide mineralizations at a depth of 200 m have been located
954 in quartzite in areas such as Brittany, and sulphide ores have been located in granite in
955 Cornwall. Above mineralizations, carbon dioxide in the soil gas has been found to
956 increase to 10% from the normal concentration of 1%. The carbon dioxide flow may
957 be as large as $0.2 \text{ l m}^{-2} \text{ h}^{-1}$ (Hermansson et al. 1991). The Dongshengmiao deposit lies
958 in a seismically active zone. The Langshan Mountain-front fault, in which minor
959 earthquake activity frequently takes place and where M=6 earthquakes have taken
960 place three times in the twentieth century, passes through the deposit. The release of
961 geogas in active tectonic areas is widespread and occurs at a significant level (Judd et
962 al., 1997; Etiope, 1999; Mörner and Etiope, 2002). The CO_2 emission flux of the
963 Siena Graben Faults (Italy), Siena G. Arbia Fault (Italy), Ustica Arso Fault (Italy), and
964 San Andreas Fault (California) were 0.83–1123, 12.4–74.4, 77.3, and 0.4–23 kg m^{-2}
965 year^{-1} respectively (Etiope, 1995; 1999; Mörner and Etiope, 2002; Lewicki and
966 Brantley, 2000). These equate, respectively, to 0.02–26.94, 0.3–1.78, 1.85, and
967 0.01–0.55 $\text{cm}^3 \text{ m}^{-2} \text{ s}^{-1}$ if CO_2 density is assumed to be 1.3401 kg m^{-3} . The area of the
968 Dongshengmiao deposit is 4.65 km^2 . The emission flux estimation of the
969 Dongshengmiao deposit was $0.5 \text{ cm}^3 \text{ m}^{-2} \text{ s}^{-1}$ according to the emission fluxes of the
970 above-mentioned faults and deposits. Therefore, the estimated degassing rate for the

971 Dongshengmiao deposit was $2.325 \text{ m}^3 \text{ s}^{-1}$.

972 The distribution areas of concealed sulfur ore deposits are different. The ore deposits
973 with the distribution areas of $1\text{--}12 \text{ km}^2$ may have more deposits than other areas.
974 Concealed metal deposits containing sulfide minerals can be very extensive, such as
975 the Killik massive sulfide deposit in northeastern Turkey (Çiftçi et al., 2005), the
976 Masa Valverde blind massive sulfide deposit in Spain (Ruiz et al., 2002), and the
977 Huize carbonate-hosted Zn–Pb–(Ag) District in South China (Han et al., 2007).
978 Concealed sulfur nonmetallic deposits, such as gypsum and barite, are also widely
979 distributed. The number of concealed sulfide deposits is far greater than those of
980 active volcanoes. Under the climate-warming conditions, oxidation of
981 sulfur-containing minerals is particularly accelerated.

982

983

984

985

986 Table S1 Plasma spectrum S results for liquid collectors along the 1st section ($\mu\text{g/mL}$)

Number	S	Number	S	Number	S	Number	S
K1-1	0.22	K1-9	0.08	K1-17	0.12	K1-25	0.43
K1-2	0.20	K1-10	0.18	K1-18	0.13	K1-26	0.33
K1-3	0.13	K1-11	0.15	K1-19	0.26	K1-27	0.83
K1-4	0.12	K1-12	0.12	K1-20	0.27	K1-28	0.15
K1-5	0.12	K1-13	0.75	K1-21	0.68	K1-29	0.48
K1-6	0.12	K1-14	0.13	K1-22	0.37	K1-30	0.09
K1-7	0.35	K1-15	0.14	K1-23	0.91	K1-31	0.09
K1-8	0.13	K1-16	0.20	K1-24	0.11		

987

988

989

990 Table S2 Plasma spectrum S results for liquid collectors along the 2nd section (µg/mL)

Number	S	Number	S	Number	S	Numer	S
K2-1	1.74	K2-20	3.81	K2-39	0.6	K2-59	0.31
K2-2	1.21	K2-21	1.52	K2-40	0.9	K2-60	0.58
K2-3	1.46	K2-22	4.44	K2-41	1.08	K2-61	0.42
K2-4	0.27	K2-23	0.72	K2-42	0.26	K2-62	0.59
K2-5	1.68	K2-24	1.07	K2-43	2.03	K2-63	3.86
K2-6	0.97	K2-25	0.57	K2-44	1.05	K2-64	0.51
K2-7	0.31	K2-26	0.43	K2-45	0.48	K2-65	0.57
K2-8	1.35	K2-27	0.61	K2-46	2.46	K2-66	0.2
K2-9	0.93	K2-28	0.11	K2-47	0.45	K2-67	0.2
K2-10	1.51	K2-29	0.39	K2-48	0.8	K2-68	0.49
K2-11	0.27	K2-30	1.39	K2-49	0.28	K2-69	0.29
K2-12	0.52	K2-31	0.88	K2-50	0.24	K2-70	0.87
K2-13	2.55	K2-32	0.6	K2-51	4.73	K2-71	0.65
K2-14	0.48	K2-33	4.63	K2-52	0.29	K2-72	0.3
K2-15	1.97	K2-34	1.84	K2-53	6.85	K2-73	8.28
K2-16	1.21	K2-35	4.1	K2-54	0.57	K2-74	0.48
K2-17	2.73	K2-36	1.92	K2-55	0.69	K2-75	1.84
K2-18	1.27	K2-37	1.18	K2-56	5.85	K2-76	
K2-19	0.22	K2-38	0.38	K2-57	0.61	K2-77	

991
992
993
994
995
996
997
998
999

1000
1001

1002 Table S3 Plasma spectrum S results for liquid collectors along the 3rd section (µg/mL)

Number	S	Number	S	Number	S	Number	S
K3-1	34.90	K3-6	19.43	K3-11	4.08	K3-16	76.28
K3-2	2.35	K3-7	1.00	K3-12	16.88	K3-17	77.21
K3-3	4.89	K3-8	1.38	K3-13	74.51	K3-18	79.81
K3-4	0.52	K3-9	1.43	K3-14	51.57	K3-19	81.52
K3-5	2.65	K3-10	0.10	K3-15	49.66	K3-20	76.07

1003
1004
1005
1006

1007

1008 **References**

1009 Çiftçi, E., Kolaylı, H., and Tokel, S.: Lead-arsenic soil geochemical study as an
1010 exploration guide over the Killik volcanogenic massive sulfide deposit,
1011 Northeastern Turkey, *J. Geochem. Explor.*, 86, 49–59, 2005.

1012 Du, L. T.: The new implication about oil-gas origin and outgassing of the earth
1013 obtained in Russia, Ukraine, Azerbaijan in new century, *Lithologic Reservoirs*,
1014 21(4), 1–9, 2009 (in Chinese with English abstract).

1015 Etiope, G.: Migrazione e comportamento del “Geogas” in bacini argillosi. Ph.D.
1016 Thesis, Dept. Earth Sciences, University of Rome “La Sapienza”, Extended
1017 abstract in *Plinius* (1996), 15, 90–94, 1995.

1018 Etiope, G.: Subsoil CO₂ and CH₄, and their advective transfer from faulted grassland
1019 to the atmosphere, *J. Geophys. Res.*, 104 (D14), 16889–16894, 1999.

1020 Han, R. S., Liu, C. Q., Huang, Z. L., Chen, J., Ma, D. Y., Lei, L., and Ma, G. S.:
1021 Geological features and origin of the Huize carbonate-hosted Zn–Pb–(Ag)
1022 District, Yunnan, South China, *Ore Geol. Rev.*, 31, 360–383, 2007.

1023 Hermansson, H.P., Akerblom, G., Chyssler, J., and Linden, A.: Geogas: A Carrier or a
1024 Tracer. SKN Report No. 51. National Board for Spent Nuclear Fuel, Stockholm,
1025 1–66, 1991.

1026 Judd, A. G., Davies, J., Wilson, J., Holmes, R., Baron, G., and Bryden, I.:
1027 Contributions to atmospheric methane by natural seepages on the UK continental
1028 shelf, *Mar. Geol.*, 137, 165–189, 1997.

1029 Lewicki, J., and Brantley, S. L.: CO₂ degassing along the San Andreas fault, Parkfield,

- 1030 California, *Geophys. Res. Lett.* 27, 5–8, 2000.
- 1031 Malmqvist, L. and Kristiansson, K.: Experimental evidence for an ascending
1032 micro-flow of geogas in the ground, *Earth Planet. Sc. Lett.*, 70, 407–423, 1984.
- 1033 Mürner, N.-A. and Etiope, G.: Carbon degassing from the lithosphere, *Global Planet.*
1034 *Change*, 33, 185–203, 2002.
- 1035 Ruiz, C., Arribas, A., and Arribas, Jr., A.: Mineralogy and geochemistry of the Masa
1036 Valverde blind massive sulphide deposit, Iberian Pyrite Belt (Spain), *Ore Geol.*
1037 *Rev.*, 19, 1–22, 2002.
- 1038 Yuan, L. L., Wang, M. Q., and Hu, J. L.: Research of geochemical gas prospecting in
1039 sunit, *Coal Technology*, 33, 85–87, 2014 (in Chinese with English abstract).
- 1040 [Wang, M. Q., Gao, Y. Y., and Liu, Y. H.: Progress in the collection of Geogas in](#)
1041 [China, *Geochem.: Explor. Environ. Anal.*, 8, 183–190, 2008.](#)
- 1042
- 1043
- 1044
- 1045
- 1046
- 1047
- 1048
- 1049
- 1050
- 1051
- 1052
- 1053
- 1054
- 1055
- 1056

1057 **The comments of an anonymous Referee #3**

1058 1. Reviewer's 1 worries are unfounded - the experimental data and the authors'
1059 procedures have been observed and employed by many, including us, and are
1060 certainly true. Their speculative ideas about "ascending gas carrying along
1061 nanoparticles 5-500 nm", I consider wrong. In addition, these "nanoparticles"
1062 penetrate through high efficiency filters, as reported in "Progress in the collection of
1063 Geogas in China", by Wang MQ, Gao YY and Liu YH, *Geochemistry: Exploration,
1064 Environment, Analysis*, vol. pp 183-190, 2008. This paper has to be cited instead of
1065 Yuan LL, Wang MQ and Hu JL, line 246 in the MS. This paper is in Chinese and not
1066 accessible on the Web of Science.

1067 2. Response to your second point, whether the authors' revisions are OK, the answer is
1068 - they are irrelevant. Here is how big the flows are: the "passive" ones are about 10^{-6}
1069 cm/s (lines 270-305). The "active" ones are, roughly, 10^7 x higher (Wang MQ et al.
1070 mentioned above). It uses a pump and reports the flow, the concentration/m³, in the
1071 flow drawn through the high efficiency filter, into their adsorber.

1072 The total flow of the "ascending flow" nanoparticles could be estimated if multiplied
1073 by the earth surface area (or the surface area of faults, if anyone knows what it is), and
1074 one ends up with enormous total flow. However, any quantification attempt is
1075 premature; the main purpose of this paper should be to establish existence of an
1076 anomaly.

1077 Another point, the authors cite a paper (line 408), Holub et al., *J. Aerosol Sci.*, 30,
1078 1999, which is appropriate - except they should also quote the essential sequel, Holub
1079 RF et al, "Further investigations...", *J. Aerosol Sci.*, 2001 to .

1080 To conclude: This paper provides an opportunity to start what's called a "paradigm
1081 shift". The first step is to acknowledge there exists an anomaly. So far numerous
1082 papers reporting this have been ignored for about 15 years.

1083 **Responses to the comments of an anonymous referee #3**

1084 1. Speculation about the mechanisms of particle transport has been minimized.
1085 "Progress in the collection of Geogas in China" by Wang, M. Q., Gao, Y. Y., and
1086 Liu, Y. H., *Geochemistry: Exploration, Environment, Analysis*, Vol. 8, pp. 183–190,
1087 2008 has been cited. Because the sulfur content of particles carried by ascending
1088 geogas flow was not mentioned in "Progress in the collection of Geogas in China"
1089 "Research of geochemical gas prospecting in sunit" by Yuan, L. L., Wang, M. Q., and
1090 Hu, J. L., *Coal Technology*, Vol. 33, pp. 85–87, 2014, has been retained.

1091 2. "Further investigations of the "geoaerosol" phenomenon" by Holub, R. F.,
1092 Hovorka, J., Reimer, G. M., Honeyman, B. D., Hopke, P. K., and Smrz P. K., *Journal
1093 of Aerosol Science*, Vol. 32, no. 1, Sup., 2001 has also been cited.

1094

1095

1096

1097 **The comments of the editor's comments**

1098 Please take into account the referee report when revising the manuscript. Especially,
1099 minimize the speculations about the mechanisms of particle transport. As you and
1100 your co-authors admit in your new Resource Geology article (which should be
1101 referenced), currently there is no good theoretical process that can explain the
1102 transport.

1103 Regarding the flow of the nanoparticles, I do not completely agree with the referee. I
1104 think that the order-of-magnitude estimate for the Dongshengmiao deposit is useful,
1105 and you can get an estimate of the sulfur emission (tons per year) if you multiply it
1106 with the sulfur content obtained from the liquid collector. Furthermore, this estimate
1107 can be compared e.g. to a typical coal-fired power plant emission. However, I think
1108 that the text relating to the estimates (lines 242-312) is too long and tedious. I suggest
1109 that you shift it to a supplement, and replace it just by giving the estimates of the
1110 sulfur contents of the geogas (1-121.5 mg/m³) and the degassing rate of the
1111 Dongshngmiao deposit (~2000M³/s), and the resulting estimate for the annual
1112 sulfur emission from the deposit.

1113 As a minor point, the sentence on lines 43-45 should be rewritten: Kiehl (1999) notes
1114 that gas phase sulfur can attach to mineral particle surfaces, but saying that "Sulfate
1115 particles... occur in mineral dust" is confusing.

1116 **Responses to editor's comments**

1117 The estimated rate of degassing for the Dongshengmiao deposit calculated to be 2.325
1118 m³ s⁻¹. The mean sulfur content of the particles carried by the ascending geogas flow
1119 for the Dongshengmiao deposit was calculated according to 45 mg/m³ (Supplement).
1120 The estimated annual sulfur emission from particles in the deposit was 3.254 tons. Qi
1121 et al. (2007) reported a flue gas amount of 527300 m³ h⁻¹ from the Huhehaote power
1122 plant in China and an exit particle concentration of 43.3 mg m⁻³ carried by the flue
1123 gas. The SO₃ distribution range in fly ash in 14 power plants (e.g., Tangshan power
1124 plant, Gaojing power plant, and Zhengzhou power plant) was reported to range
1125 between 0 and 1.05 %. The mean SO₃ and sulfur contents in fly ash were 0.27 % and
1126 0.108 %, respectively. On the basis of these mean values, 21.305 tons of annual
1127 particulate sulfur emission occurred from the flue gas in the Huhehaote power plant.
1128 The annual sulfur emission from the particles carried by ascending geogas flow in the
1129 Dongshengmiao deposit was less than carried by the flue gas in the Huhehaote power
1130 plant. However, the amount of concealed deposits is much more than that of
1131 coal-burning power plants. Moreover, size of the particles carried by the ascending
1132 geogas flow from concealed deposits is usually <500 nm. The mean diameter of the
1133 particles carried by the flue gas in 9 samples obtained from four coal-fired power
1134 plants in China were 19.71, 3.18, 5.43, 5.67, 130.94, 77.29, 12.99, 11.59, and 236.63
1135 μm respectively (Zhang et al. 2007). The sizes of particles carried by the ascending
1136 geogas flow from concealed deposits were lesser than those of the particles carried by
1137 the flue gas from coal-fired power plants. Within a certain volume, the particles were
1138 smaller and the number of particles was more. These small particles are more capable

1139 of migration and have a significant health and environmental impact. Therefore,
1140 attention must be paid to the particles carried by the ascending geogas flow from
1141 concealed deposits.

1142 In addition, the sentence on lines 43–45 has been revised. Speculation about the
1143 mechanisms of particle transport has been minimized. Lines 242–312 have been
1144 moved to a supplementary section.

1145 References

1146 Qi, L. Q., Yuan, Y. T., and Liu, J.: Current situations of emission and collection on fly
1147 ash of power plants in China: International Conference on Power Engineering-2007,
1148 Hangzhou, China, 23 – 27 October 2007, 766 – 772, 2007.

1149 Zhang, C. F., Yao, Q., and Sun, J. M.: Characteristics of particulate matter from
1150 emissions of four typical coal-fired power plants in China, *Fuel Process Technol.*, 86,
1151 757– 768, 2005.

1152

1153

1154 Author's changes in manuscript

1155 P. 3, line 45: “, occur in mineral dust (Kiehl, 1999)” has been deleted.

1156

1157 P. 4, line 58: “, 2001” has been added.

1158

1159 P. 10, line 211: “. Because gases and particles move along faults, they can migrate
1160 over long distances” has been deleted.

1161

1162 P. 11, line 222: “the particles or particle aggregations were found in ascending geogas
1163 flows in faults at different depths near or above the concealed ore bodies of the
1164 Dongshengmiao polymetallic sulfide deposit. This observation demonstrates that the
1165 faults are channels for particles carried by the ascending geogas flow.” was deleted.

1166

1167 P. 12, line 250: “For 16 ore deposits, in which we have studied particles carried by
1168 ascending geogas, a large number of sulfur-containing and Pb- and As-containing
1169 particles were found. There are oxidative ore bodies in many concealed sulfide ore
1170 deposits. As sulfide minerals change into oxide minerals, sulfide was released from
1171 these minerals. There are some sulfide concentration data for ascending geogas. Yuan
1172 et al. (China University of Geosciences, Beijing, China, 2014) analyzed sulfide
1173 concentrations of ascending geogas in soil at the Sunit deposit (the Inner Mongolia
1174 Autonomous Region, China), using plasma mass spectrographic analysis. Their
1175 sampling method allowed the flow of geogas in the soil through liquid collector
1176 slowly using a pump. The particles carried by the ascending geogas flow were
1177 adsorbed in the liquid collector. The volume of the geogas extracted per hole was 5
1178 liters. The geogas extracted from 3 holes (15 liters) was combined to make one
1179 sample. The liquid collector was made with high purity nitric acid and Mini-Q ultra
1180 pure water. The liquid collector was placed in a 25 ml polyethylene bottle. The

1181 analysis results from 1054 samples showed that the average sulfur content of the
1182 liquid collector was $26.4571 \mu\text{g ml}^{-1}$. The maximum value was $35.33 \mu\text{g ml}^{-1}$ and the
1183 minimum value was $16.89 \mu\text{g ml}^{-1}$. A concentration of $26.4571 \mu\text{g ml}^{-1}$ in the liquid
1184 collector may be translated into 44.095 mg per cubic meter of geogas flow. We know
1185 that sulfur-containing substances carried by geogas flow may be not completely
1186 adsorbed in the liquid collector. Therefore, the average sulfur content of the ascending
1187 geogas flow may have been higher than 44.095 mg per cubic meter. We analyzed the
1188 sulfide concentration of ascending geogas in the soil at the Kangjiawan deposit in the
1189 Hunan Province, China. Our sampling method is similarly to the method used by
1190 Yuan et al. (2014). The main difference is that our liquid collector was made with
1191 high purity aqua regia and tri-distilled water. The volume of the liquid collector was
1192 100 ml. The volume of the geogas extracted from a hole was 9 liters. Therefore, the
1193 volume of the geogas extracted from 3 holes was 27 liters. The sulfide concentration
1194 of the liquid collector was analyzed using the plasma spectrum method. We analyzed
1195 the samples along 3 sections (sample numbers were 31, 74, and 20). The results
1196 showed that the average sulfur contents of the 3 sections were 0.27, 1.40, and 32.81
1197 $\mu\text{g ml}^{-1}$ respectively (Tables 4–6), which may be translated into 1.00, 5.19, and
1198 121.50 mg per cubic meter of geogas flow, respectively. There is earth degassing
1199 phenomena in metallic and nonmetallic deposits. The giant gold deposits, such as the
1200 Porcupine gold deposit in Canada, the Witwatersrand gold deposit in South Africa,
1201 and the Muruntau gold deposit in Uzbekistan, exhibit upward vertical movement of
1202 hydrocarbon gas. The Witwatersrand gold deposit has significant upward gas flow. In
1203 one day, 36700 m^3 of hydrocarbon gases degas from underground gold mining vents
1204 and $5 \times 10^8 \text{ m}^3$ of hydrocarbon gases degas from 3000m or deeper mines every year.
1205 The Azerbaijan oil and gas region is strongly degassed, with $4 \times 10^8 \text{ m}^3$ of gases
1206 degassed every year (Du, 2009). The ascending gas flow rates were measured to be
1207 between 60×10^{-4} and $4 \text{ cm}^3 \text{ min}^{-1} \text{ m}^{-2}$ horizontally projected borehole area at three
1208 different sites by Malmqvist & Kristiansson (1984). Carbon dioxide concentrations
1209 above sulfide mineralizations are often enhanced. Hidden sulfide mineralizations at a
1210 depth of 200 m have been located in quartzite in areas such as Brittany, and sulphide
1211 ores have been located in granite in Cornwall. Above mineralizations, carbon dioxide
1212 in the soil gas has been found to increase to 10% from the normal concentration of 1%.
1213 The carbon dioxide flow may be as large as $0.2 \text{ l m}^{-2} \text{ h}^{-1}$ (Hermansson et al. 1991).
1214 The Dongshengmiao deposit lies in a seismically active zone. The Langshan
1215 Mountain-front fault, in which minor earthquake activity frequently takes place and
1216 where M=6 earthquakes have taken place three times in the twentieth century, passes
1217 through the deposit. The release of geogas in active tectonic areas is widespread and
1218 occurs at a significant level (Judd et al., 1997; Etiope, 1999; Mörner and Etiope,
1219 2002). The CO_2 emission flux of the Siena Graben Faults (Italy), Siena G. Arbia Fault
1220 (Italy), Ustica Arso Fault (Italy), and San Andreas Fault (California) were 0.83–1123,
1221 12.4–74.4, 77.3, and 0.4–23 $\text{kg m}^{-2} \text{ year}^{-1}$ respectively (Etiope, 1995; 1999; Mörner
1222 and Etiope, 2002; Lewicki and Brantley, 2000). These equate, respectively, to
1223 0.02–26.94, 0.3–1.78, 1.85, and 0.01–0.55 $\text{cm}^3 \text{ m}^{-2} \text{ s}^{-1}$ if CO_2 density is assumed to be
1224 1.3401 kg m^{-3} . The area of the Dongshengmiao deposit is 4.65 km^2 . The emission flux

1225 estimation of the Dongshengmiao deposit was $0.5 \text{ cm}^3 \text{ m}^{-2} \text{ s}^{-1}$ according to the
1226 emission fluxes of the above-mentioned faults and deposits. Therefore, the estimated
1227 degassing rate for the Dongshengmiao deposit was $2.325 \text{ m}^3 \text{ s}^{-1}$. The distribution
1228 areas of concealed sulfur ore deposits are different. The ore deposits with the
1229 distribution areas of $1\text{--}12 \text{ km}^2$ may have more deposits than other areas. Concealed
1230 metal deposits containing sulfide minerals can be very extensive, such as the Killik
1231 massive sulfide deposit in northeastern Turkey (Çiftçi et al., 2005), the Masa
1232 Valverde blind massive sulfide deposit in Spain (Ruiz et al., 2002), and the Huize
1233 carbonate-hosted Zn–Pb–(Ag) District in South China (Han et al., 2007). Concealed
1234 sulfur nonmetallic deposits, such as gypsum and barite, are also widely distributed.
1235 The number of concealed sulfide deposits is far greater than those of active volcanoes.
1236 Under the climate-warming conditions, oxidation of sulfur-containing minerals is
1237 particularly accelerated.” has been moved to a supplementary section.

1238 “The estimated rate of degassing for the Dongshengmiao deposit calculated to be
1239 $2.325 \text{ m}^3 \text{ s}^{-1}$. The mean sulfur content of the particles carried by the ascending geogas
1240 flow for the Dongshengmiao deposit was calculated according to 45 mg/m^3
1241 (Supplement). The estimated annual sulfur emission from particles in the deposit was
1242 3.254 tons. Qi et al. (2007) reported a flue gas amount of $527300 \text{ m}^3 \text{ h}^{-1}$ from the
1243 Huhehaote power plant in China and an exit particle concentration of 43.3 mg m^{-3}
1244 carried by the flue gas. The SO_3 distribution range in fly ash in 14 power plants
1245 (e.g., Tangshan power plant, Gaojing power plant, and Zhengzhou power plant) was
1246 reported to range between 0 and 1.05 %. The mean SO_3 and sulfur contents in fly ash
1247 were 0.27 % and 0.108 %, respectively. On the basis of these mean values, 21.305
1248 tons of annual particulate sulfur emission occurred from the flue gas in the Huhehaote
1249 power plant. The annual sulfur emission from the particles carried by ascending
1250 geogas flow in the Dongshengmiao deposit was less than carried by the flue gas in the
1251 Huhehaote power plant. However, the amount of concealed deposits is much more
1252 than that of coal-burning power plants. Moreover, size of the particles carried by the
1253 ascending geogas flow from concealed deposits is usually $<500 \text{ nm}$. The mean
1254 diameter of the particles carried by the flue gas in 9 samples obtained from four
1255 coal-fired power plants in China were 19.71, 3.18, 5.43, 5.67, 130.94, 77.29, 12.99,
1256 11.59, and $236.63 \text{ }\mu\text{m}$ respectively (Zhang et al. 2007). The sizes of particles carried
1257 by the ascending geogas flow from concealed deposits were lesser than those of the
1258 particles carried by the flue gas from coal-fired power plants. Within a certain volume,
1259 the particles were smaller and the number of particles was more. These small particles
1260 are more capable of migration and have a significant health and environmental impact.
1261 Therefore, attention must be paid to the particles carried by the ascending geogas flow
1262 from concealed deposits. ” has been added.

1263
1264 P. 14, line 415: “have high migration ability and” has been deleted.

1265
1266 P. 15, line 433–P. 20, line 604: “Çiftçi, E., Kolaylı, H., and Tokel, S.: Lead-arsenic
1267 soil geochemical study as an exploration guide over the Killik volcanogenic massive
1268 sulfide deposit, Northeastern Turkey, *J. Geochem. Explor.*, 86, 49–59, 2005.”, “Du, L.

1269 T.: The new implication about oil-gas origin and outgassing of the earth obtained in
1270 Russia, Ukraine, Azerbaijan in new century, *Lithologic Reservoirs*, 21(4), 1–9, 2009
1271 (in Chinese with English abstract).”, “Etioppe, G.: Migrazione e comportamento del
1272 “Geogas” in bacini argillosi. Ph.D. Thesis, Dept. Earth Sciences, University of Rome
1273 “La Sapienza”, Extended abstract in *Plinius* (1996), 15, 90–94, 1995.”, “Etioppe, G.:
1274 Subsoil CO₂ and CH₄, and their advective transfer from faulted grassland to the
1275 atmosphere, *J. Geophys. Res.*, 104 (D14), 16889–16894, 1999.”, “Han, R. S., Liu, C.
1276 Q., Huang, Z. L., Chen, J., Ma, D. Y., Lei, L., and Ma, G. S.: Geological features and
1277 origin of the Huize carbonate-hosted Zn–Pb–(Ag) District, Yunnan, South China, *Ore
1278 Geol. Rev.*, 31, 360–383, 2007.”, “Hermansson, H.P., Akerblom, G., Chyssler, J., and
1279 Linden, A.: Geogas: A Carrier or a Tracer. SKN Report No. 51. National Board for
1280 Spent Nuclear Fuel, Stockholm, 1–66, 1991. ”, “Judd, A. G., Davies, J., Wilson, J.,
1281 Holmes, R., Baron, G., and Bryden, I.: Contributions to atmospheric methane by
1282 natural seepages on the UK continental shelf, *Mar. Geol.*, 137, 165–189, 1997.
1283 Lewicki, J., and Brantley, S. L.: CO₂ degassing along the San Andreas fault, Parkfield,
1284 California, *Geophys. Res. Lett.* 27, 5–8, 2000.”, “Malmqvist, L. and Kristiansson, K.:
1285 Experimental evidence for an ascending micro-flow of geogas in the ground, *Earth
1286 Planet. Sc. Lett.*, 70, 407–423, 1984.”, “Mörner, N.-A. and Etioppe, G.: Carbon
1287 degassing from the lithosphere, *Global Planet. Change*, 33, 185–203, 2002.”, “Ruiz,
1288 C., Arribas, A., and Arribas, Jr., A.: Mineralogy and geochemistry of the Masa
1289 Valverde blind massive sulphide deposit, Iberian Pyrite Belt (Spain), *Ore Geol. Rev.*,
1290 19, 1–22, 2002.”, “Yuan, L. L., Wang, M. Q., and Hu, J. L.: Research of geochemical
1291 gas prospecting in sunit, *Coal Technology*, 33, 85–87, 2014 (in Chinese with English
1292 abstract).” have been moved to a supplementary section.
1293
1294 P. 16, line 472: “Holub, R. F., Hovorka, J., Reimer, G. M., Honeyman, B. D., Hopke,
1295 P. K., and Smrz P. K.: Further investigations of the "geoaerosol" phenomenon, *J.
1296 Aerosol Sci.*, 32, 61–70, 2001.” has been added.
1297
1298 P. 18, line 545: “Qi, L. Q., Yuan, Y.T., and Liu, J.: Current situations of emission and
1299 collection on fly ash of power plants in China: International Conference on Power
1300 Engineering-2007, Hangzhou, China, 23 – 27 October 2007, 766 – 772, 2007.” has
1301 been added.
1302
1303 P. 20, line 599: “Zhang, C. F, Yao, Q., and Sun, J. M.: Characteristics of particulate
1304 matter from emissions of four typical coal-fired power plants in China, *Fuel Process
1305 Technol.*, 86, 757– 768, 2005.” has been added.
1306
1307 P. 38, line 836: Table 4–6 have been moved to a supplementary section.
1308
1309 P. 41, line 937: “Wang et al. (2008) collected particles carried by ascending geogas in
1310 soil over the Jiaolongzhang Pb-Zn-Cu-Ag deposit, Eastern Gansu, China using a
1311 liquid collector. Analysis results from 14 samples showed that the mean content of Cu,
1312 Pb, and Zn was 844 ng/ml (gas volume), 107 ng/ml, and 1751 ng/ml, respectively.”

1313 has been added.

1314

1315 P. 46, line 1040: “Wang, M. Q., Gao, Y. Y., and Liu, Y. H.: Progress in the collection
1316 of Geogas in China, *Geochem.: Explor. Environ. Anal.*, 8, 183–190, 2008.” has been
1317 added.

1318

1319

1320

1321

1322

1323

1324

1325

1326

1327